Organic & Biomolecular Chemistry

ROYAL SOCIETY OF CHEMISTRY

PAPER

View Article Online
View Journal

Cite this: DOI: 10.1039/d6ob00422a

Diastereoselective synthesis of 1,4,8-trisubstituted perhydroquinolines as novel κ receptor agonists

Lea Flämig,[a] W. Felix Zhu,[a] Katharina Hoffmann,[b] Constantin Daniliuc,[c] Dirk Schepmann,[a] Frank Glorius,[c] Marcel Bermúdez,[a,d] Karin Loser[b] and Bernhard Wünsch *[a,d]

Agonists of the κ-opioid receptor are useful drugs for the treatment of severe pain, itching skin diseases and inflammatory and immunological diseases. Herein, novel κ agonists with the κ-pharmacophoric ethylenediamine system embedded in a rigid decahydroquinoline scaffold (**6**) were designed, synthesized and pharmacologically evaluated. The synthesis of decahydroquinolines **6** consisted of three parts: (1) synthesis of 4,8-disubstituted tetrahydroquinolines **14**; (2) diastereoselective hydrogenation of tetrahydroquinolines **14** to afford decahydroquinolines **17**; and (3) stereoselective introduction of the pyrrolidine ring at the 8-position and various acyl moieties at the 1-position. The dichlorophenylacetyl and fluorophenylacetyl derivatives **6a** (K_i = 86 nM) and **6b** (K_i = 134 nM) showed considerably lower κ affinity than the lead compounds **4** (K_i = 0.81 nM) and **5** (K_i = 0.25 nM). In docking studies, the NH moiety of the exocyclic carbamates **6a** and **6b** served as an H-bond donor towards the OH moiety of Y239, whereas the methoxycarbonyl moiety of endocyclic carbamate **5** formed a beneficial H-bond with the NH backbone of L212. The lower κ affinity of **6a** and **6b** was at least partially compensated by increased polarity, leading to promising LLE values of 5.69 and 6.87, respectively. Both κ agonists **6a** and **6b** revealed high selectivity over μ- and δ-opioid receptors and high metabolic stability in the presence of mouse liver microsomes and NADPH. The anti-inflammatory activity of the κ receptor agonist **6a** was investigated with human peripheral blood mononuclear cells stimulated with lipopolysaccharide, and the effects were compared with those of the lead compounds **4** and **5**. Methyl carbamate **6a** exhibited the smallest reduction in pro-inflammatory monocyte subsets and did not affect cytokine secretion. It was concluded that **6a** had a substantially weaker anti-inflammatory activity than the lead compounds **4** and **5**.

Received 13th March 2026,
Accepted 12th May 2026

DOI: 10.1039/d6ob00422a

rsc.li/obc

1. Introduction

The κ-opioid receptor, belonging to the class of G protein-coupled receptors, is found in the central nervous system and also in keratinocytes of the skin and immune cells.[1] Agonists of the κ opioid receptor can be used for the treatment of severe pain as well as itching skin diseases, such as atopic dermatitis, psoriasis and severe pruritus associated with kidney failure.[2] Furthermore, κ receptor agonists can be useful to ameliorate inflammatory and immunological diseases including multiple sclerosis.[3,4]

The first synthetic κ opioid receptor agonist is U-50488 (**1**). Its pharmacophore consists of ethylenediamine with one N atom embedded in a pyrrolidine ring and the other one in a dichlorophenylacetamide moiety. Its high κ receptor affinity (K_i = 0.89 nM)[8] translates into strong analgesic activity. Very high κ affinity can be achieved by introduction of these κ pharmacophoric elements into a piperidine ring (**2**) and a piperazine ring (**3**, GR-89696). The piperidine and piperazine derivatives **2** and **3** show slightly higher κ affinity (K_i (**2**) = 0.24 nM,[9] K_i (**3**) = 0.46 nM[10]) than the cyclohexane derivative U-50488 (**1**) (Fig. 1).

In the κ agonist **4**, the cyclohexane ring of U-50488 (**1**) and the piperidine ring of **2** are annulated, resulting in a *cis*-configured decahydroquinoline. The high κ affinity of **4** (K_i = 0.81 nM) resulted in strong effects on the immune system. The amount of inflammatory immune cells and the release of pro-inflammatory cytokines were reduced.[5] *cis*-Annulation of the piperazine ring of **3** and the cyclohexane ring of **1** provided the decahydroquinoxaline **5**, which also showed high κ affinity (K_i = 0.25 nM).[6,7] In addition to its high κ affinity, **5** showed anti-inflammatory and

[a]*Universität Münster, Institut für Pharmazeutische und Medizinische Chemie, Corrensstraße 48, D-48149 Münster, Germany. E-mail: wuensch@uni-muenster.de; Tel: +49-251-8333311*
[b]*Universität Oldenburg, Fakultät für Medizin und Gesundheitswissenschaften, Carl-von-Ossietzky-Straße 9-11, Gebäude W16/W37, D-26129 Oldenburg, Germany*
[c]*Universität Münster, Organisch-Chemisches Institut, Corrensstraße 40, D-48149 Münster, Germany*
[d]*Universität Münster, GRK 2515, Chemical biology of ion channels (Chembion), Corrensstraße 48, D-48149 Münster, Germany*

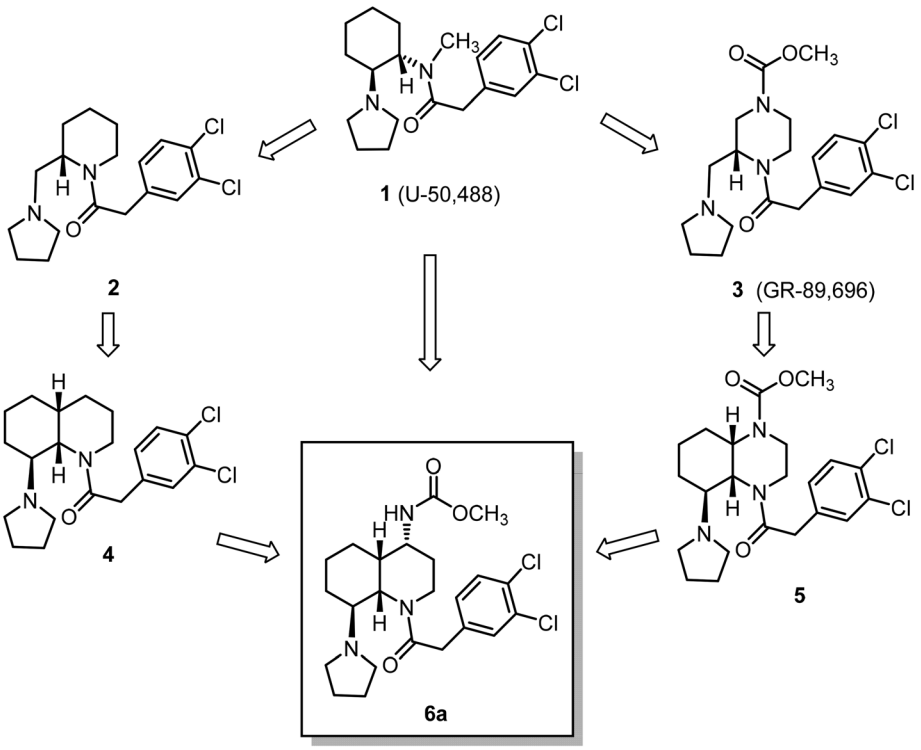

Fig. 1 Development of κ receptor agonist **6a** as a hybrid of perhydroquinoline **4** (K_i = 0.81 nM)[5] and perhydroquinoxaline **5** (K_i = 0.25 nM).[6,7]

immunomodulatory properties in two mouse models and exhibited promising anti-itching and anti-inflammatory activity. In a combined phase 1/2 clinical study, **5** could ameliorate itching in patients suffering from atopic dermatitis. Although the κ agonist was applied topically, a few patients reported sedative effects. As sedation is a typical centrally mediated side effect of κ agonists, the clinical study was discontinued (Fig. 1).

Herein, we report on the development of a novel chemotype **6** (Fig. 1), which should address the κ receptor with high affinity. The key pharmacophoric elements are retained in **6**, but the decoration of the bicyclic heterocycle is modified. In **6a**, a methyl carbamate is attached to the perhydroquinoline system of **4**. This methyl carbamate is a substructure of the decahydroquinoxaline **5**, but its N atom is not included in the heterocyclic system and is instead attached to the decahydroquinoline scaffold. The shift of the complete methyl carbamate outside the ring system results in a larger diversity, *i.e.*, the exocyclic N-atom of **6** can be substituted with two substituents, allowing fine-tuning of its pharmacodynamic and pharmacokinetic properties. Moreover, the *cis*- and *trans*-orientations of the substituent on the decahydroquinoline system represent a further dimension of diversity.

2. Results and discussion

2.1. Diastereoselective synthesis of decahydroquinoline 6 and analogs

The synthesis of decahydroquinoline **6** comprises three parts: first, two substituents were introduced at the 4- and 8-positions to obtain tetrahydroquinolines **14a–d**. The key step in the synthesis was the diastereoselective hydrogenation of the pyridine ring of **14a–d** to afford decahydroquinolines **17a–d**. Finally, the κ-pharmacophoric structural elements were introduced at the 8-position (pyrrolidine ring) and the 1-position (3,4-dichlorophenylacetyl moiety).

In order to introduce two substituents at the 4- and 8-positions of the quinoline ring, tetrahydroquinoline (**7**) was converted into the *N*-oxide **8** with *m*-chloroperbenzoic acid (*m*CPBA).[5] Nitration of **8** with HNO_3/H_2SO_4 provided the nitro derivative **9** in 65% yield. Böckelheide rearrangement of the *N*-oxide **9** with Ac_2O led to the rearranged acetate **10**, which was hydrolyzed with NaOH to afford alcohol **11** in 51% yield (from **9**). After protection of alcohol **11** as the TBS ether **12**, reduction of the NO_2 moiety with H_2 and Pd/C led to the primary amine **13**, which was acylated to obtain amides **14b** and **14d** and carbamate **14c**. Methyl carbamate **14a** was prepared by reaction of the primary amine **13** with CDI and subsequently with methanol (Scheme 1).

Initial attempts to reduce tetrahydroquinoline **14** with H_2 and Pd/C failed to give decahydroquinolines **17**. Therefore, a stepwise reduction of the tetrahydroquinoline ring of **14** was conducted. Benzylation of **14b–d** with benzyl bromide provided the benzylpyridinium bromides **15b–d**, which were reduced with $NaBH_4$ to afford the octahydroquinolines **16b–d**. The last double bond of **16b–d** was diastereoselectively hydrogenated from the side opposite to the large TBSO moiety, providing **17b–d** with the four protons at the 4-, 4a-, 8-, and 8a-

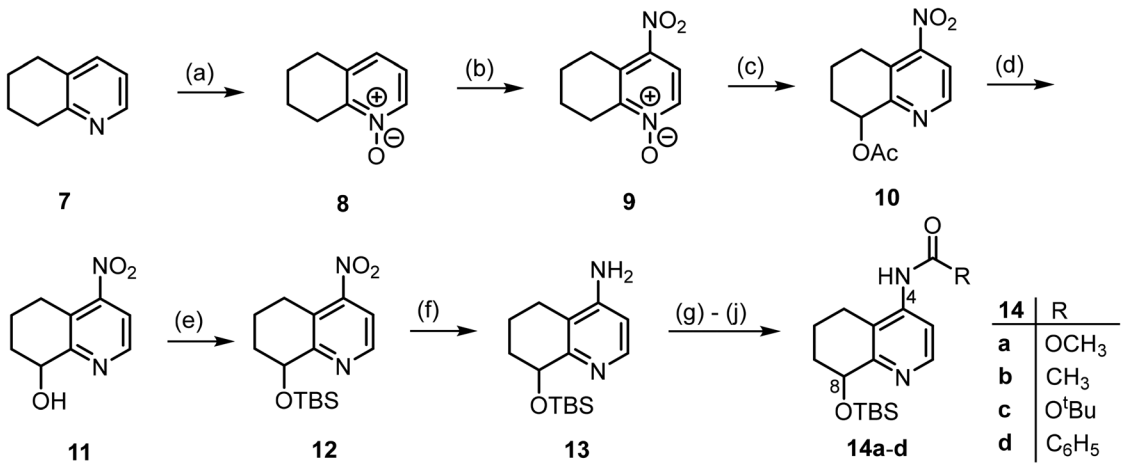

Scheme 1 Modification of tetrahydroquinoline (**7**) at the 4 and 8-positions. Reagents and reaction conditions: (a) *m*CPBA, CH_2Cl_2, rt, 24 h, 81%. (b) Conc. H_2SO_4, fuming HNO_3, 0 °C to 50 °C, 30 min, 65%. (c) Ac_2O, 120 °C, 1 h. (d) NaOH (1 M), rt, 1 h, 51% (from **9**). (e) TBS-Cl, imidazole, DMAP, CH_2Cl_2, rt, 18 h, 93%. (f) H_2 (1 bar), Pd/C, EtOH, rt, 1 h, 99%. (g) 1. CDI, DMAP, CH_3CN, 82 °C, 5 h; 2. CH_3OH, 80 °C, 72 h, 84% (**14a**). (h) Ac_2O, 60 °C, 3 h, 99% (**14b**). (i) Boc_2O, NEt_3, CH_2Cl_2, 40 °C, 18 h, 43% (**14c**). (j) Benzoyl chloride, NEt_3, CH_2Cl_2, CH_3CN, rt, 22 h, 78% (**14d**).

positions on the same side of the decahydroquinoline ring (Scheme 2).

Although decahydroquinolines **17b–d** were accessible through this three-step sequence, the whole process including purification was labor-intensive and time-consuming. Moreover, the yields of the final hydrogenation step leading to decahydroquinolines **17c** (36%) and **17d** (34%) were rather low. Therefore, the direct hydrogenation of tetrahydroquinolines **14** using different catalysts under high pressure was re-investigated (for exhaustive reviews on arene hydrogenation, see ref. 11 and 12). Using Pd/C or $Pd(OH)_2/C$, hydrogenation of benzamide **14d** even at 50 bar and 50 °C for 2–3 days and addition of HCl or HOAc failed to afford decahydroquinoline **17d**. Low conversion of acetamide **14b** was observed with H_2 in

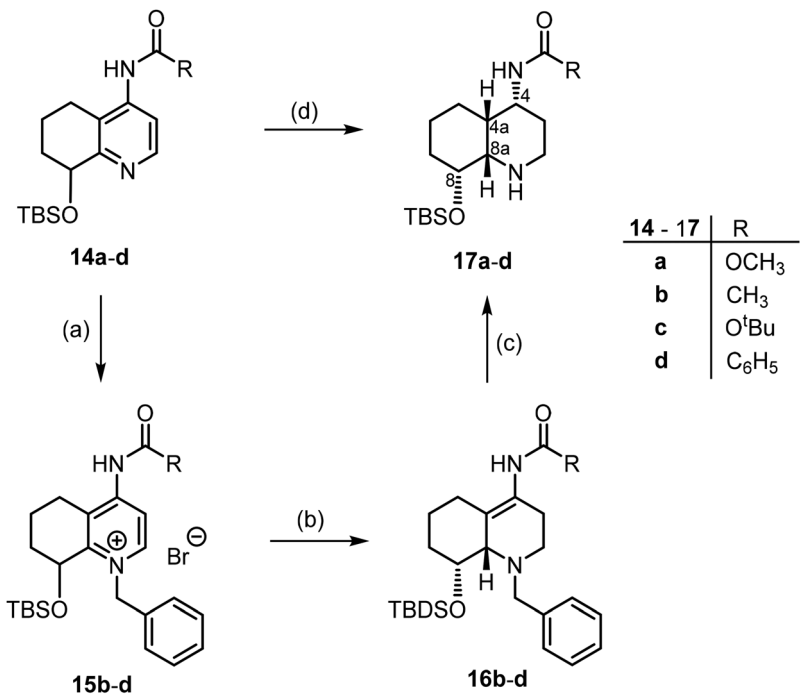

Scheme 2 Synthesis of decahydroquinolines **17a–d** by reduction/hydrogenation of the pyridine ring. Reagents and reaction conditions: (a) BnBr, CH_3CN, 40–45 °C, 40–94 h, 74–100%. (b) $NaBH_4$, CH_3OH, rt, 3.5–22.5 h, 54–80%. (c) H_2 (5 bar), Pd/C, Ch_3OH, rt, 60–120 h, 36% (**17c**), 34% (**17d**). (d) H_2 (50 bar), Ru/C, AcOH, iso-PrOH, 80 °C, 42 h, 72% (**17a**), 77% (**17b**). Only one enantiomer of the racemic mixtures **16** and **17** is shown, respectively.

the presence of PtO_2 (50 bar, 80 °C, 2–3 d, HOAc additive), whereas full conversion was observed with Rh_2O_3/PtO_2 and Ru/C under the same conditions. After hydrogenation of **14a** and **14b** with Ru/C at 50 bar and 80 °C (42 h, solvent isopropanol/HOAc), decahydroquinolines **17a** and **17b** were isolated in 72% and 77% yields, respectively (Scheme 2). The relative configurations of **17a** and **17b**, *i.e.*, the orientation of the four methine protons at the 4-, 4a-, 8a-, and 8-positions on the same side of the decahydroquinoline system, were carefully analyzed by NOE spectroscopy (see Fig. S2 in the SI) and were later confirmed using the crystal structure of the final product **6a**·HCl.

In order to achieve high *cis*-stereoselectivity, the OH moiety at the 8-position was protected with the large TBS group, which directs the transfer of H_2 from the opposite side. As a result, the protons at the four centers of chirality at the 4-, 4a-, 8a-, and 8-positions are located on the same side of the decahydroquinoline plane in **17a**. It is assumed that the pyridine ring interacts with the catalyst surface, which leads to the transfer of H_2 to one side of the pyridine ring opposite to the large OTBS group.

The third part of the synthesis consisted of the conversion of the OTBS moiety into a pyrrolidine ring with inversion of configuration and the acylation of the decahydroquinoline *N*-atom. For this purpose, the silyl ether of **17a** was cleaved with TBAF and the resulting β-amino alcohol **18** was reacted with SO_2Cl_2 to obtain the cyclic sulfuric acid ester amide **19** in 49% yield. In **19**, the secondary alcohol is activated for an S_N2 substitution, and simultaneously, the secondary amine is protected. The S_N2 reaction of **19** with pyrrolidine provided the substitution product **20** with inversion of configuration at the 8-position. Finally, acylation of the secondary amine **20** with various acid derivatives led to amides **6a–d**. The (3,4-dichlorophenyl)acetamide **6a** was prepared by acylation of the secondary amine **20** with the corresponding acid chloride **21a**, whereas NHS-esters **21b–d** were used for the introduction of the acyl moieties in **6b–d**. The structures and syntheses of the NMS esters **21b–d** are provided in the SI, part 3. The (3,4-dichlorophenyl)acetyl moiety of **6a** represents the standard acyl moiety for achieving high κ receptor affinity. In **6b** and **6c**, the 3,4-dichlorophenyl moiety is replaced by a 4-fluorophenyl and a pyridin-3-yl moiety, respectively. In **6d**, the (3,4-dichlorophenyl)acetyl moiety is shortened to a 3,4-dichlorobenzoyl moiety (Scheme 3).

Unexpectedly, the same reaction sequence starting from acetamide **17b** resulted in such low yields that the transformation could not be completed to yield the final (3,4-dichlorophenyl)acetamide with sufficient purity. The low yields were due to the high polarity of the intermediates making isolation and purification very difficult.

In order to prove the desired relative configuration of the final products **6**, an X-ray crystal structure of the HCl salt of (3,4-dichlorophenyl)acetamide **6a** was obtained. The crystal structure of **6a**·HCl showed the pairwise *cis*-configuration of the protons 4-H/4a-H and 4a-H/8a-H, thus confirming the *cis*-configuration of the decahydroquinoline scaffold. Moreover,

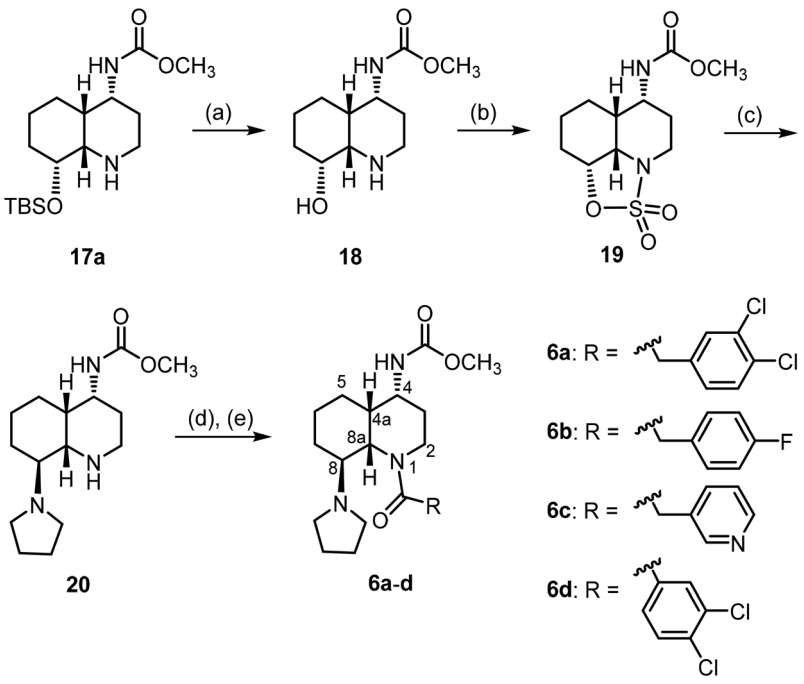

Scheme 3 Introduction of the κ pharmacophoric structural elements to finalize the synthesis of κ receptor agonists **6a–d** with a decahydroquinoline scaffold. Reagents and reaction conditions: (a) TBAF, THF, rt, 20 h, 100%. (b) SO_2Cl_2, NEt_3, CH_3CN, rt, 60 h, 49%. (c) Pyrrolidine, CH_3CN, 80 °C, 48 h, 65%. (d) 2-(3,4-Dichlorophenyl)acetyl chloride (**21a**), DIPEA, THF, rt, 18 h, 49% (**6a**). (e) NHS-esters **21b–d** (for synthesis, see the SI, part 3), Na_2CO_3 (5% in H_2O), THF, rt, 18 h or 72 h, 36% (**6b**), 40% (**6c**), 13% (**6d**). Only one enantiomer of the racemic mixtures **17–20** and **6** is shown, respectively.

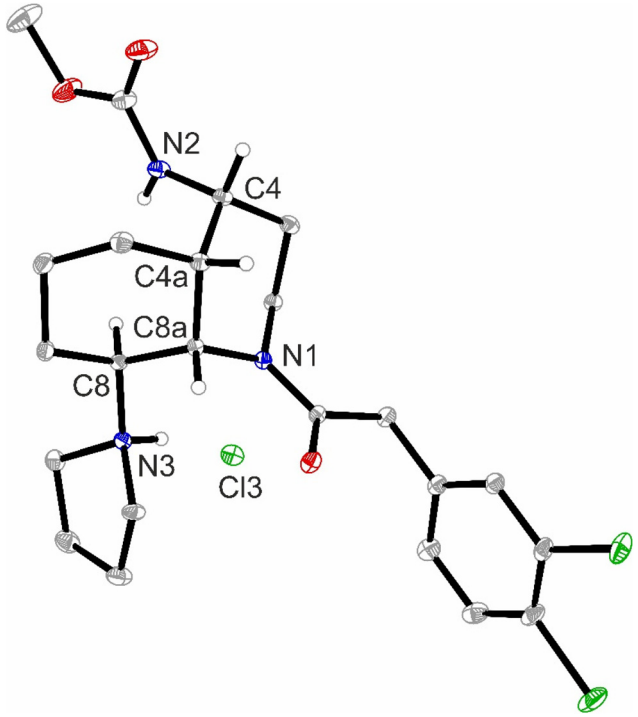

Fig. 2 X-ray crystal structure of decahydroquinoline **6a**·HCl. For clarity, hydrogen atoms were omitted, with the exception of those located at the C atoms of centers of chirality and NH groups. The structure proves the *cis*-orientation of the protons at the 4-, 4a-, and 8a-positions as well as the inversion of configuration at the 8-position during the S_N2 substitution with pyrrolidine. The *cis*-configuration of the decahydroquinoline ring system is confirmed.

the inverted configuration at the 8-position due to the S_N2 reaction with pyrrolidine is shown by the *trans*-configuration of the protons at the 8- and 8a-positions. The dihedral angle (N1–C8a–C8–N3) is 53.7(2)° (Fig. 2). It was hypothesized that the relative orientation of the pyrrolidine ring and the dichlorophenylacetyl moiety defined by the dihedral angle (N1–C8a–C8–N3) is crucial for high κ-opioid receptor affinity.

2.2. Pharmacological evaluation of decahydroquinolines 6a–d

Radioligand receptor binding studies were used to determine the interactions of decahydroquinolines **6a–d** with κ-, μ-, and δ-opioid receptors as well as σ_1 and σ_2 receptors. The affinity for σ receptors was included, as small structural modifications of κ ligands can shift the affinity profile from κ to σ receptors and *vice versa*.[13] In the κ assay, tritium-labeled [^{3}H]U-69593 was employed as the radioligand and membrane preparations from guinea pig brains were used as the receptor material. The same receptor material was used in the μ ([^{3}H]DAMGO) and σ_1 ([^{3}H]-(+)-pentazocine) assays. Rat brain and rat liver membrane preparations served as the receptor material in the δ assay ([^{3}H]DPDPE) and the σ_2 assay ([^{3}H]di-*o*-tolylguanidine), respectively.[6,14–16] The recorded affinities of **6a–d** together with the affinity data of reference compounds are summarized in Table 1.

The κ affinity of methyl carbamate **6a** (K_i = 86 nM) substituted with the prototypical κ-pharmacophoric dichlorophenylacetyl moiety is considerably lower than the κ affinity of the lead compounds **1–5** (see Table 1 and Introduction). The reduced κ affinity of **6a** compared to the unsubstituted decahydroquinoline **4** (K_i = 0.81 nM) was attributed to the additional methoxycarbonylamino moiety at the 4-position. The outward shift of the methyl carbamate from decahydroquinoxaline **5** (K_i = 0.25 nM) might be the reason for the reduced κ affinity of **6a**.

Replacement of the dichlorophenyl moiety of **6a** with a fluorophenyl moiety slightly reduced the κ affinity of **6b**, whereas the pyridin-3-yl substituent of **6c** eliminated the κ affinity almost completely. Removal of the CH_2 spacer between the carbonyl moiety and the phenyl ring led to a 3-fold reduction in the κ affinity of benzamide **6d** compared to phenylacetamide **6a**.

Dichlorophenylacetamide **6a** and fluorophenylacetamide **6b** showed high selectivity towards the related μ- and δ-opioid receptors as well as σ_1 and σ_2 receptors. In contrast, dichlorobenzamide **6d** exhibited almost the same affinity for κ and μ receptors and only 2-fold selectivity for κ over the *δ* receptor.

2.3. Molecular docking of decahydroquinolines 5, 6a, and 6b

The proposed binding modes of decahydroquinoline derivatives **5**, **6a**, and **6b** indicate highly similar binding orientations, and the ligands display similar key interactions with the active κ-receptor binding pocket. Most importantly, a salt bridge between D138 and ionizable nitrogen, reported to be crucial to recognize κ-receptor agonists, is observed for all docked compounds (Fig. 3). All docked ligands also form a hydrogen bond with Q115. The dichlorophenyl moiety of **5** shows lipophilic contacts with W124 similar to those of **6a**, but the lipophilic surface of **6b** is smaller due to the mono-substitution with a F atom at the 4-position. The largest difference in receptor–ligand interactions could be observed for the methyl carbamate moiety, in which the N atom of **6a** and **6b** serves as a hydrogen-bond donor and forms a hydrogen bond with Y139. While the N atom of **5** is part of the ring structure, the methyl carbamate of **5** displays a hydrogen bond with L212. Although the number of hydrogen bonds is equal, the direct interaction with L212 as part of extracellular loop 2 might be considered beneficial for stabilizing the active receptor–ligand complex. The general orientations and key interactions of available co-resolved κ receptor agonists including MP1104 (PDB ID: 6B73)[17] and U-50488 (PDB ID: 9W49)[18] support our proposed binding modes for decahydroquinoline derivatives (see Fig. S3 in the SI) and are consistent with recent docking-based binding-mode studies.[19–22]

2.4. Physicochemical and pharmacokinetic characterization of decahydroquinolines 6

In order to reduce the failure of drugs *in vivo* or during clinical studies, drug candidates should be characterized carefully with respect to their physicochemical and pharmacokinetic properties as early as possible during drug development. The

Table 1 Affinity of decahydroquinolines **6a–d** and reference compounds at κ receptors and related opioid and σ receptors

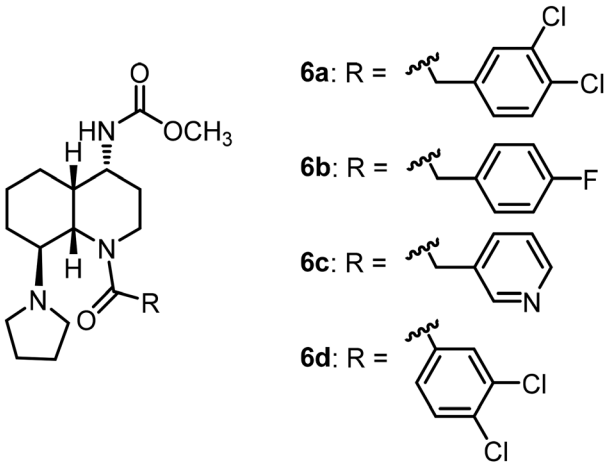

Compd	K_i ± SEM[a,b] [nM]				
	κ receptor [^{3}H]U-69593	μ receptor [^{3}H]DAMGO	δ receptor [^{3}H]DPDPE	σ_1 receptor [^{3}H]-(+)-Pentazocine	σ_2 receptor [^{3}H]DTG[c]
4	0.81 ± 0.32	7%	0%	676	3300
5	0.25 ± 0.08	43 ± 9.2	58 ± 8.4	n.d.	n.d.
6a	86 ± 8	1100	866	0%	0%
6b	134 ± 50	2000	0%	0%	0%
6c	0%	0%	0%	0%	0%
6d	278 ± 17	217	672	0%	0%
U-50488 (**1**)	0.34 ± 0.07	—	—	—	—
U-69593	0.88 ± 0.10	—	—	—	—
Naloxone	6.9 ± 0.5	2.3 ± 1.1	103	—	—
Morphine	35 ± 6	5.2 ± 1.6	—	—	—
SNC80	—	—	1.2 ± 0.5	—	—
(+)-Pentazocine	—	—	—	5.4 ± 0.5	—
Haloperidol	—	—	—	6.6 ± 0.9	78 ± 2

[a] K_i values with SEM values represent the mean of three independent experiments (n = 3). K_i values without SEM values represent the result of one experiment. Values in % express the inhibition of the radioligand binding at a test compound concentration of 1 μM. [b] Guinea pig brain membrane preparations were used in the κ, μ and σ_1 assays. In the δ assay, rat brain, and in the σ_2 assay, rat liver membrane preparations were used. [c] DTG = di-*o*-tolylguanidine.

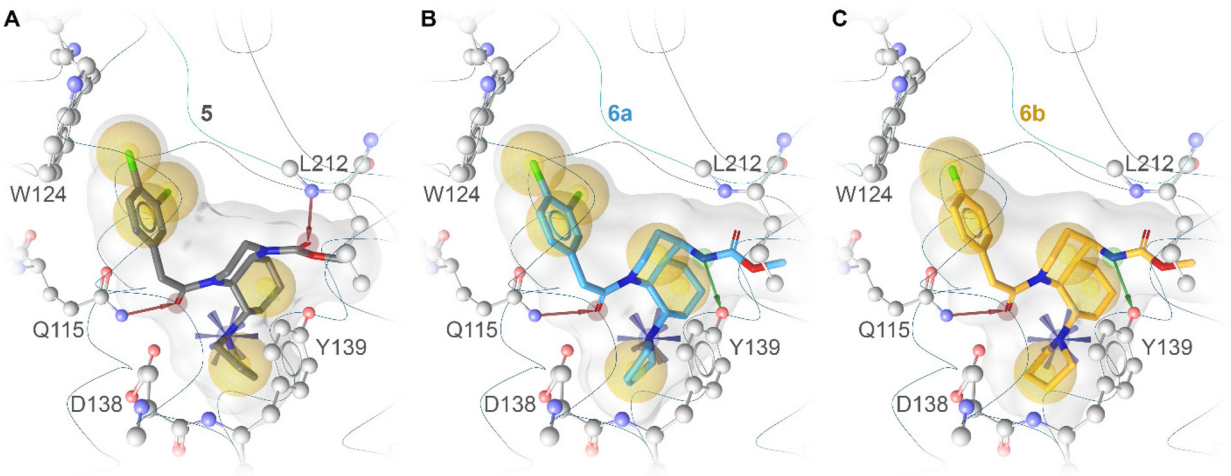

Fig. 3 Proposed binding modes of decahydroquinoline derivatives **5** (A), **6a** (B), and **6b** (C) at the active κ receptor obtained by docking (PDB ID: 6B73).[17] Ligand–receptor interactions are illustrated by a blue star (with the positive ionizable center forming a salt bridge with conserved D138), yellow spheres (lipophilic contacts), red arrows (hydrogen bond acceptors), and green arrows (hydrogen bond donors). The ligand molecular surface is depicted in semitransparent grey.

Table 2 Physicochemical and pharmacokinetic properties including ligand-lipophilicity efficiency (LLE) of decahydroquinolines **6**

Compd	$-\log K_i$ (κ affinity)	$\log D_{7.4}$ ± SD (n = 3)	LLE[a]	Plasma protein binding ± SD (n = 3)[b]	Metabolic stability ± SD (n = 3)[c]
6a	7.07	1.38 ± 0.07	5.69	79 ± 0.1%	92 ± 2.2%
6b	6.87	0.0 ± 0.05	6.87	50 ± 0.3%	92 ± 1.8%
6c	—	−0.42 ± 0.12	—	43 ± 1.2%	89 ± 4.7%
6d	6.56	1.66 ± 0.04	4.90	79 ± 0.3%	93 ± 2.2%
Imipramine	—	—	—	—	20%

[a] LLE (ligand-lipophilicity efficiency) = $-\log K_i - \log D_{7.4}$. [b] Interaction with human serum albumin was determined by HPAC analysis. [c] The amount (in %) of the parent compound remaining after incubation with mouse liver microsomes and NADPH for 90 min.

recorded physicochemical and pharmacokinetic parameters are summarized in Table 2.

2.4.1 Lipophilicity ($\log D_{7.4}$ value) and LLE. For this purpose, the $\log D_{7.4}$ values of decahydroquinolines **6a–d** were determined using the micro shake-flask method. After distribution of the test compound between a MOPS buffer pH 7.4 layer and an *n*-octanol layer, the amount of the compound in the buffer layer was determined by MS. Since MS leads to a very low limit of quantification, 0.5–0.8 mg of the test compound is already sufficient to obtain reliable $\log D_{7.4}$ values.[23,24]

The recorded $\log D_{7.4}$ value of 1.38 promises optimal pharmacokinetic behavior of dichlorophenylacetamide **6a**. Replacement of the dichlorophenyl moiety of **6a** with a fluorophenyl (**6b**) or pyridyl moiety (**6c**) increased the polarity remarkably up to $\log D_{7.4}$ = 0.0 (**6b**) and −0.42 (**6c**). Elimination of the CH_2 spacer resulted in increased lipophilicity of benzamide **6d** with $\log D_{7.4}$ = 1.66 (Table 2).

The ligand–lipophilicity efficiency (LLE) value reflects the modulation of the biological activity of a drug by its lipophilicity. With the help of this value, it can be evaluated, whether the biological activity is caused by lipophilic obesity of the drug candidate. LLE is defined as $-\log K_i - \log D_{7.4}$.[25,26] In Table 2, the LLE values of decahydroquinolines **6** are displayed. Due to its high polarity (low lipophilicity), the fluorophenyl derivative **6b** exhibits the highest LLE value of 6.87, which exceeds the $\log D_{7.4}$ value of the dichlorophenylacetyl derivative **6a** by more than one log unit. The low LLE value of benzamide **6d** (4.90) is a result of its low κ affinity and relatively high lipophilicity. It can be concluded that the LLE values of both dichlorophenylacetamide **6a** and fluorophenylacetamide **6b** are in a promising range above 5.0 (Table 2).

2.4.2 Plasma protein binding. The plasma protein binding (PPB) was determined by high-performance affinity chromatography (HPAC). In this chromatographic system, the stationary phase was coated with human serum albumin, which is predominantly responsible for the transportation of small and large compounds in human blood.[23,27,28] The recorded retention time correlated with the affinity of the drugs for human serum albumin. The measured PPB matched well with the polarity of the κ agonists **6**: the more polar ligands **6c** and **6b** show rather low PPB (43% and 50%), whereas the more lipophilic candidates **6a** and **6d** revealed higher PPB of 79% each (Table 2).

2.4.3 Metabolic stability. Especially for the translation into animal experiments, metabolic stability represents a key feature of novel drugs. The metabolic stability of decahydroquinolines **6a–d** was recorded upon incubation with mouse liver microsomes and NADPH for 90 min at 37 °C. Under these conditions, transformation *via* CYP enzymes is observed predominantly, which represents the most important liver enzymes responsible for the oxidative biotransformation of xenobiotics.[23,29] After an incubation period of 90 min, more than 89% of the parent compounds remained unchanged, indicating very high metabolic stability (Table 2).

2.4.4 Blood–brain barrier permeability. Finally, an *in vitro* assay to assess the passive blood–brain barrier (BBB) permeability of κ agonists **4**, **5**, **6a**, and **6b** was conducted. The blood–brain barrier-specific parallel artificial membrane permeability assay (PAMPA-BBB) is a good predictor of passive diffusion of drugs across the BBB.[30–32] In this assay, a 96-well membrane filter plate was coated with a porcine brain lipid extract solution and the extent of diffusion through this membrane was quantified by LC-MS to calculate the effective permeability coefficient P_e. A higher $\log P_e$ coefficient correlates with a higher *in vivo* log BB value (BB is defined as the ratio of the drug concentration in the brain to the drug concentration in the blood).

In this assay, compounds **6a** and **6b** exhibited significantly reduced $\log P_e$ values compared to compounds **4** and **5**, which is in good agreement with their lower lipophilicity, higher total polar surface area (TPSA) and higher number of hydrogen-bond acceptor and donor groups (Table 3).

Table 3 Permeability of the blood–brain barrier determined in the PAMPA-BBB assay for selected κ receptor ligands and diazepam as the reference compound

Compd	$\log P_e$ [a]	MR[b] (%)	MW (g mol^{-1})	TPSA[c]	HBA/HBD[d]
4	−4.39 ± 0.02	0.43 ± 0.05	395.4	23.6 Å^2	2/0
5	−4.50 ± 0.05	0.21 ± 0.06	454.4	53.1 Å^2	4/0
6a	−4.65 ± 0.03	0.19 ± 0.03	468.4	61.9 Å^2	4/1
6b	−4.97 ± 0.02	0.01 ± 0.05	417.5	61.9 Å^2	5/1
Diazepam	−4.35 ± 0.05	0.28 ± 0.09	284.7	32.67 Å^2	2/0

[a] $\log P_e$ = decimal logarithm of the effective permeability coefficient (n = 3). [b] MR = membrane retention factor. [c] TPSA (total polar surface area) calculated using SwissADME.[33] [d] HBA = number of hydrogen bond acceptors; HBD = number of hydrogen bond donors.

2.5. Effects of 4, 5 and 6a on human monocytes

Monocytes play a central role in the initiation and regulation of inflammatory responses. Circulating monocytes originate from bone marrow precursors and can rapidly migrate to sites of tissue injury or infection, where they differentiate into macrophages or dendritic cells and contribute to pathogen clearance, antigen presentation, and cytokine production.[34,35] Human monocytes are commonly classified into three subsets based on the expression of CD14 and CD16: classical ($CD14^{+}CD16^{-}$), intermediate ($CD14^{+}CD16^{+}$), and non-classical ($CD14^{dim}CD16^{+}$) monocytes. Classical monocytes, representing the majority of circulating monocytes, are primarily involved in acute inflammatory responses, whereas intermediate and non-classical monocytes exhibit enhanced antigen-presenting capacity, patrol along the vascular endothelium and thereby contribute to immune surveillance.[36,37] Moreover, non-classical and intermediate monocytes are known for their ability to secrete high levels of pro-inflammatory cytokines.

κ-Opioid receptor expression has been detected in all primary human monocyte subsets, with particularly high expression reported in intermediate and non-classical monocytes.[38] Upon activation, the κ receptor triggers intracellular signaling cascades involving the suppression of adenylate cyclase and the inhibition of downstream pathways including nuclear factor-κB (NF-κB). Accordingly, stimulation of the κ receptor with agonists like U-50488 (**1**) down-regulated the lipopolysaccharide- (LPS-) induced inflammatory response by preventing the translocation of the NF-κB p65 subunit into the nucleus, finally resulting in the reduction of pro-inflammatory cytokine production, including TNF, IL-1, and IL-6.[38,39]

The functional impact of κ receptor signaling might differ between monocyte subsets. Given the higher expression of the receptor in intermediate and non-classical monocytes, these populations may be particularly sensitive to κ receptor-mediated immunomodulation. Both intermediate and non-classical monocytes are often associated with chronic inflammatory diseases. Thus, κ agonists may preferentially suppress their activity and pharmacological targeting of the κ receptor could represent a useful strategy for modulating monocyte-driven inflammation in pathological conditions such as arthritis, autoimmune diseases, and chronic infections.[36,40,41]

To investigate this aspect in more detail, we isolated monocytes from the peripheral blood of healthy human donors, activated them with LPS and stimulated them with the κ agonists **4**, **5** and **6a**. As shown in Fig. 4, all three compounds were able to significantly down-regulate the number of non-classical as well as intermediate monocytes, whereas the κ agonists had a minor effect on $CD14^{+}CD16^{-}$ classical monocytes. Notably, the effect of compound **4** was the most pronounced, whereas compound **6a** had the least effect on the reduction of the pro-inflammatory monocyte subsets (Fig. 4).

Since it is known that the κ agonist U-50488 (**1**) suppresses inflammatory responses in LPS-stimulated cells by inhibiting NF-κB activation, thereby leading to the reduction of TNF,

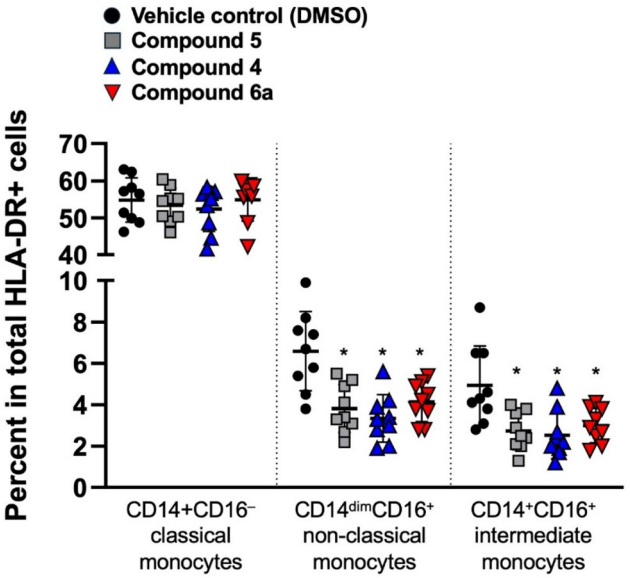

Fig. 4 κ Agonists **4**, **5** and **6a** significantly reduced the number of pro-inflammatory non-classical and intermediate monocytes. Total human antigen-presenting cells were isolated from buffy coat blood, activated for 12 h with LPS (1 μg mL^{-1}), and stimulated with κ agonists **4**, **5** and **6a** at a concentration of 10 μM for an additional 4 days. Control cells received an equal amount of DMSO (vehicle control). Percentages of classical, non-classical and intermediate monocytes within total antigen-presenting cells from n = 9 healthy donors are shown. Cells are gated for HLA-DR+ singlets and data are presented as mean ± SEM; *$p < 0.05$.

IL-6 or IL-1 release, we next investigated the cytokine secretion in LPS-activated human monocytes following stimulation with compounds **4**, **5** and **6a**. As expected, compound **4** exerted a pronounced anti-inflammatory effect since treatment with compound **4** significantly inhibited the secretion of the pro-inflammatory cytokines IL-1, TNF, and IL-6 in cultures of activated monocytes (Fig. 5A). Consistent with prior expectations (Loser, unpublished data), compound **5** also displayed anti-inflammatory potential, as indicated by a trend towards reduced IL-1, TNF, and IL-6 secretion in LPS-stimulated monocytes compared with vehicle-treated control cells, although these effects did not reach statistical significance. In contrast, stimulation of activated monocytes with compound **6a** did not affect cytokine secretion, suggesting that the anti-inflammatory activity of this compound is substantially weaker than that observed for the two reference compounds (Fig. 5A).

During inflammatory activation, monocytes undergo functional and phenotypic changes beyond the secretion of pro-inflammatory cytokines. In addition to releasing IL-1, IL-6 and TNF, activated monocytes up-regulate surface molecules including CD44 or CD69. CD44, a transmembrane glycoprotein, promotes cell trafficking to inflamed tissues. At the sites of inflammation, activated monocytes contribute to the induction of adaptive immune responses and thereby participate in the perpetuation of inflammatory processes.[42] CD69 is a rapid, early activation marker and triggering CD69

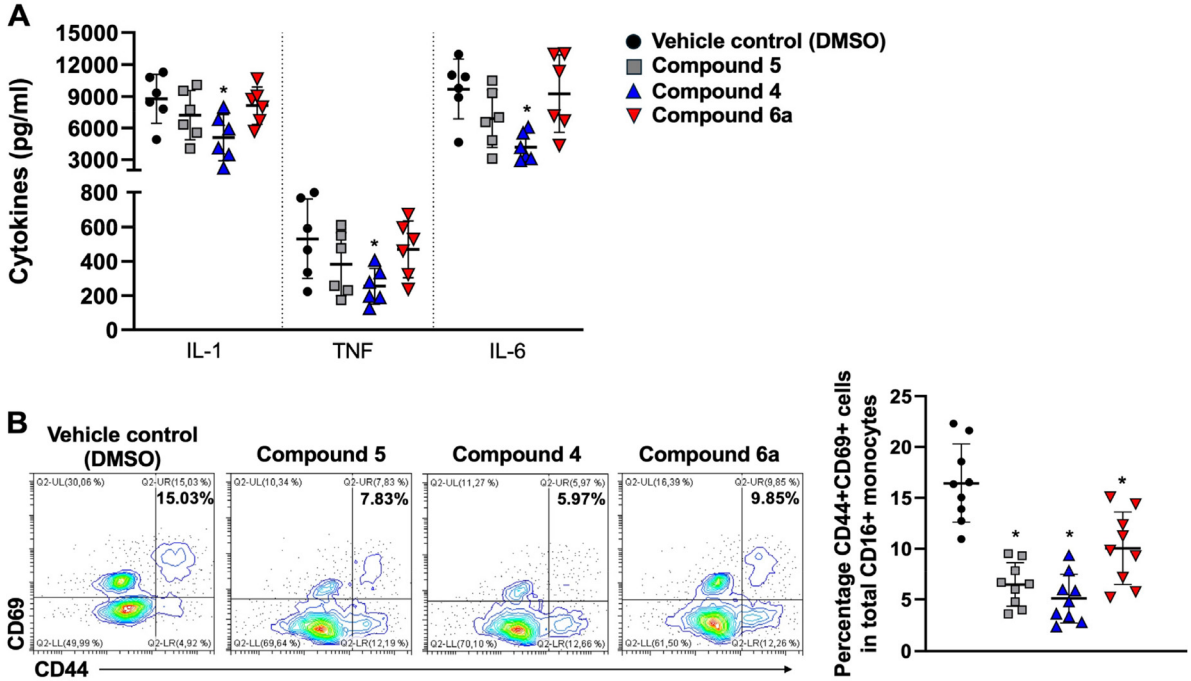

Fig. 5 Compound **4** reduced the secretion of pro-inflammatory cytokines and all compounds were able to block the expression of activation markers on the surface of activated non-classical and intermediate monocytes. (A) Isolated human $CD16^+$ monocytes were activated with LPS for 12 h and subsequently stimulated with compounds **4**, **5** and **6a** at a concentration of 10 μM for an additional 96 h. Control cells received an equal amount of the vehicle DMSO. Cytokine concentrations were quantified in cell culture supernatants using multiplex assays and the levels of the pro-inflammatory cytokines IL-1, TNF, and IL-6 are shown. Data from n = 6 healthy human donors are depicted and are presented as mean ± SEM; *p < 0.05. (B) Compounds **4**, **5** and **6a** down-regulated the expression of the activation markers CD44 and CD69. After isolation from peripheral blood, human $CD16^+$ monocytes were treated with LPS for 12 h and stimulated with the κ-agonists **4**, **5** and **6a** for 4 days. Control cells received DMSO. Representative contour plots showing the percentages of $CD44^{hi}CD69^+$ cells representing highly activated monocytes (left) and the statistical evaluation from n = 9 healthy human donors (right) are shown. Data are presented as mean ± SEM; *p < 0.05.

induces a strong pro-inflammatory response in monocytes, including the production of cytokines and reactive oxygen species.

LPS-stimulated monocytes treated with compounds **4** and **5** showed a marked reduction in the expression of the activation markers CD44 and CD69, further supporting the pronounced anti-inflammatory properties of these compounds. In comparison, treatment with compound **6a** led only to a modest decrease in the expression of these classical activation markers. Although this reduction was statistically significant relative to vehicle-treated control cells, the magnitude of the effect was considerably smaller than that observed for compounds **4** and **5** (Fig. 5B). Notably, compound **6a** did not exert detectable anti-inflammatory or immunomodulatory effects on T or B lymphocytes and failed to significantly reduce the activation of neutrophils or NK cells (data not shown). Together, these findings indicate that while compounds **4** and **5** show potent anti-inflammatory properties consistent with previously reported data (Martin *et al.*[5] and Soeberdt *et al.*[43]), compound **6a** displayed only minor anti-inflammatory potential, suggesting limited relevance of this compound for further development in more complex experimental systems such as advanced co-culture or organoid models aimed at translational applications.

3. Conclusion

The key structural elements of the potent κ agonists **4** and **5** are combined in the novel κ agonists **6**. Decahydroquinolines **6** with a methoxycarbonylamino moiety at the 4-position result from the addition of this moiety to the decahydroquinoline framework of **4** or from shifting of the N atom of the carbamate moiety from inside the decahydroquinoxaline system in **5** to an exocyclic position in **6**. The key idea of the attachment of the methoxycarbonylamino moiety to the ring system in **6** was the increase of diversity, since the exocyclic amino moiety can be provided with two substituents, allowing fine-tuning of the pharmacodynamic and pharmacokinetic properties.

Decahydroquinolines **6** were prepared by a 12-step linear synthesis. The key steps of the synthesis comprise the diastereoselective high-pressure hydrogenation (50 bar) of tetrahydroquinolines **14** using Ru/C as a catalyst and the S_N2 substitution (inversion of configuration) of the cyclic sulfuric acid ester amide **19** with pyrrolidine, leading to the desired relative configuration of the four centers of chirality in **6**.

Compared to the lead compounds **4** and **5**, the κ affinity is considerably decreased from subnanomolar affinity for **4** and **5** to K_i values of 86 nM for **6a** and 134 nM for **6b**. However, it should be considered that the K_i values of **6** refer to racemic

mixtures, whereas **4** and **5** represent the eutomers. Moreover, the relative orientation and the substitution pattern of the secondary carbamate at the 4-position can be further modified to modulate the pharmacodynamic and pharmacokinetic properties. The lower κ affinity of **6a** and **6b** was explained by the missing H-bond interaction of the methoxycarbonyl moiety of **5** with the NH backbone of L212. Instead, an H-bond between the secondary carbamates of **6a** and **6b** was formed with the OH moiety of Y139. Both ligands **6a** and **6b** showed high selectivity over μ- and δ-opioid receptors as well as σ_1 and σ_2 receptors.

Due to the secondary carbamate moiety, both κ agonists exhibit rather low lipophilicity, leading to promising LLE values of 5.69 (**6a**) and 6.83 (**6b**). Incubation of **6a** and **6b** with mouse liver microsomes and NADPH resulted in high metabolic stability, since 92% of the intact parent compound was detected after an incubation period of 90 min. The increased polarity, TPSA and the number of HBD/HBA of dichlorophenylacetamide **6a** and fluoroacetamide **6b** compared to **4** and **5** resulted in reduced passive blood–brain barrier permeability, as measured by PAMPA. This property might be exploited to develop κ agonists acting predominantly in the periphery, *e.g.*, for the treatment of itching skin diseases. Such types of κ agonists might decrease the risk of side effects resulting from targeting κ receptors in the central nervous system, including sedation, dysphoria and diuresis.

To investigate the anti-inflammatory activity of κ agonist **6a**, monocytes from the peripheral blood of healthy donors were collected, activated with LPS and stimulated with κ agonists **4**, **5**, and **6a**. All three κ agonists were able to down-regulate the number of particular monocyte subsets, but **6a** showed the weakest effect in the reduction of pro-inflammatory monocyte subsets. In contrast to κ agonists **4** and **5**, ligand **6a** could not reduce the secretion of pro-inflammatory cytokines. Treatment with κ agonist **6a** led only to a modest decrease in the expression of the classical activation markers CD44 and CD69. Altogether, κ agonist **6a** displayed only weak anti-inflammatory potential, which correlates with its reduced κ receptor affinity compared to the lead compounds **4** and **5**.

4. Experimental section

General chemistry methods including HPLC methods used to show the purity of all compounds are given in the SI. Unless otherwise mentioned, the purity of all test compounds is greater than 95%.

4.1. Synthetic procedures

4.1.1 5,6,7,8-Tetrahydroquinoline-1-oxide (8)[5]

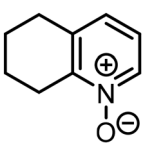

8

Under a N_2 atmosphere, *m*CPBA (419 mg, 2.4 mmol, 1.2 eq.) was added to a solution of 5,6,7,8-tetrahydroquinoline (**7**, 266 mg, 2.0 mmol, 1.0 eq.) in dry CH_2Cl_2 (16 mL) and the solution was stirred at rt for 24 h. The reaction mixture was washed with aqueous saturated solutions of $Na_2S_2O_3$ (20 mL) and $NaHCO_3$ (20 mL). The combined aqueous layers were extracted with CH_2Cl_2 (3 × 50 mL). The combined organic layers were dried (Na_2SO_4) and filtered, and the solvent was removed under reduced pressure. The crude product was purified by flash column chromatography (25 g cartridge, CH_2Cl_2/CH_3OH 98/2 → 92/8). Colorless solid, mp 72 °C, yield 241 mg (81%). $C_9H_{11}NO$ (149.2 g mol^{-1}). TLC: R_f = 0.25 (CH_2Cl_2/CH_3OH 95/5). HR-MS (APCI): *m*/*z* = 150.0932 (calcd 150.0913 for $C_9H_{12}NO^+$ $[M + H]^+$). ^{1}H NMR (400 MHz, $CDCl_3$): δ (ppm) = 1.72–1.81 (m, 2H, 6-CH_2), 1.85–1.94 (m, 2H, 7-CH_2), 2.76 (t, *J* = 6.2 Hz, 2H, 5-CH_2), 2.93 (t, *J* = 6.6 Hz, 2H, 8-CH_2), 6.96–7.05 (m, 2H, 3-H, 4-H), 8.13 (d, *J* = 6.7 Hz, 1H, 2-H). ^{13}C NMR (151 MHz, $CDCl_3$): δ (ppm) = 21.8 (C-6) 22.0 (C-7), 24.8 (C-8), 28.8 (C-5), 122.1 (C-3),126.3 (C-4), 136.5 (C-4a),137.0 (C-2), 148.9 (C-8a). FT-IR: $\tilde{\nu}$ [cm^{-1}] = 3310 (C–$H_{arom.}$), 1439 (C–$H_{aliph.}$), 1250 (N^+–O^-), 795 (=C–H_{deform}). Purity (HPLC): 98% (t_r = 12.1 min).

4.1.2 4-Nitro-5,6,7,8-tetrahydroquinoline-1-oxide (9)

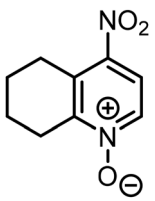

9

N-Oxide **8** (0.508 g, 3.35 mmol) was added to a mixture of conc. H_2SO_4 (5 mL) and fuming conc. HNO_3 (5 mL) at 0 °C. The mixture was stirred at 50 °C in a preheated oil bath for 30 min and afterwards poured into ice water. NaOH (5 M) was added until the solution changed color from yellow to dark orange and became alkaline. The solution was extracted with $CHCl_3$ (4 × 150 mL), the CH_3Cl layer was dried (Na_2SO_4) and filtered, and the solvent was removed under reduced pressure. The crude product was purified by flash column chromatography (25 g cartridge, cyclohexane/ethyl acetate 50/50 → 40/60). Yellow solid, mp 116 °C, yield 0.425 g (65%). $C_9H_{10}N_2O_3$ (194.2 g mol^{-1}). TLC: R_f = 0.29 (CH_2Cl_2/CH_3OH 50/1). HR-MS (APCI): *m*/*z* = 195.0769 (calcd 195.0764 for $C_9H_{11}N_2O_3^+$ $[M + H]^+$). ^{1}H NMR (400 MHz, $CDCl_3$): δ (ppm) = 1.83–1.77 (m, 2H, 6-CH_2), 1.89–1.95 (m, 2H, 7-CH_2), 2.93 (t, *J* = 6.6 Hz, 2H, 8-CH_2), 3.10 (t, *J* = 6.3 Hz, 2H, 5-CH_2), 7.80 (d, *J* = 7.2 Hz, 1H, 3-H), 8.18 (d, *J* = 7.0 Hz, 1H, 2-H). ^{13}C NMR (151 MHz, $CDCl_3$): δ (ppm) = 20.7 (C-7), 21.2 (C-6), 25.9 (C-8), 26.7 (C-5), 118.4 (C-3), 132.3 (C-4a), 137.2 (C-2), 143.2 (C-4), 151.7 (C-8a). FT-IR: $\tilde{\nu}$ [cm^{-1}] = 3101 (C–$H_{arom.}$), 1516 (NO_2), 1335 (NO_2), 1281 (N^+–O^-). Purity (HPLC): 100% (t_r = 13.3 min).

4.1.3 4-Nitro-5,6,7,8-tetrahydroquinolin-8-ol (11)

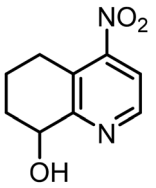

11

A solution of nitro *N*-oxide **9** (3.79 g, 19.5 mmol) in acetic anhydride (50 mL) was stirred at 120 °C for 1 h to produce acetate **10**. Acetic anhydride was removed under vacuum and aqueous NaOH (1 M, 80 mL) was added. The suspension was stirred at rt for 5 h, acidified with HCl (1 M, 90 mL) and extracted with ethyl acetate. The combined organic layers were dried (Na_2SO_4) and filtered, and the solvent was removed under reduced pressure. The crude product was purified by flash column chromatography (30 g RP cartridge, water/acetonitrile 95/5 → 0/100). Brown solid, mp 73 °C (decomp.), yield 1.94 g (51%). $C_9H_9N_2O_3$ (194.2 g mol^{-1}). TLC: R_f = 0.52 (ethyl acetate/cyclohexane 80/20). HR-MS (APCI): *m*/*z* = 195.0779 (calcd 195.0764 for $C_9H_{10}N_2O_3^+$ [M + H]$^+$). ^{1}H NMR (400 MHz, $CDCl_3$): δ (ppm) = 1.77–1.89 (m, 2H, 6-CH_{ax}, 7-CH_{ax}), 2.02–2.13 (m, 1H, 6-CH_{eq}), 2.29–2.38 (m, 1H, 7-CH_{eq}), 2.98–3.10 (m, 2H, 5-CH_2), 3.94 (s, broad, 1H, O*H*), 4.71–4.78 (m, 1H, 8-H), 7.61 (d, *J* = 5.3 Hz, 1H, 3-H), 8.66 (d, *J* = 5.1 Hz, 1H, 2-H). ^{13}C NMR (151 MHz, $CDCl_3$): δ (ppm) = 18.8 (C-6), 25.5 (C-5), 29.7 (C-7), 69.4 (C-8), 116.1 (C-3), 125.2 (C-4a), 148.1 (C-2), 155.0 (C-4), 162.6 (C-8a). FT-IR: $\tilde{\nu}$ [cm^{-1}] = 3364 (O–H), 2874 ($CH_{aliph.}$), 1531 (NO_2), 1231 (NO_2), 845 (=CH_{deform}). Purity (HPLC): 98.5% (t_r = 11.5 min).

4.1.4 8-(*tert*-Butyldimethylsilyloxy)-4-nitro-5,6,7,8-tetrahydroquinoline (12)

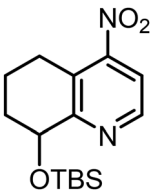

12

DMAP (6 mg, 0.05 mmol, 0.1 eq.), imidazole (173 mg, 2.36 mmol, 2.5 eq.), and TBS-Cl (192 mg, 1.04 mmol, 1.1 eq.) were added to a solution of alcohol **11** (184 mg, 0.945 mmol, 1.0 eq.) in CH_2Cl_2 (2.3 mL) and the reaction mixture was stirred at rt for 18 h. The solvent was removed under reduced pressure and the crude product was purified by flash column chromatography (10 g cartridge, cyclohexane/ethyl acetate 90/10 → 70/30). Pale yellow oil, yield 271 mg (93%). $C_{15}H_{24}N_2O_3Si$ (308.5 g mol^{-1}). TLC: R_f = 0.61 (cyclohexane/ethyl acetate 90/10). HR-MS (APCI): *m*/*z* = 309.1635 (calcd 309.1629 for $C_{15}H_{25}N_2O_3Si^+$ [M + H]$^+$). ^{1}H NMR (400 MHz, $CDCl_3$): δ (ppm) = 0.07 (s, 3H, Si-CH_3), 0.21 (s, 3H, Si-CH_3′), 0.88 (s, 9H, C(CH_3)$_3$), 1.78–1.84 (m, 1H, 6-CH_2), 1.87–1.93 (m, 1H, 7-CH_2), 2.04–2.13 (m, 2H, 6-CH_2, 7-CH_2), 2.86–2.93 (m, 1H, 5-CH_2), 3.00–3.06 (m, 1H, 5-CH_2), 4.88 (t, *J* = 4.0 Hz, 1H, 8-H), 7.53 (d, *J* = 5.1 Hz, 1H, 3-H), 8.64 (d, *J* = 5.2 Hz, 1H, 2-H). ^{13}C NMR (151 MHz, $CDCl_3$): δ (ppm) = −4.6 (*C*H_3), −3.8 (*C*H_3), 16.7 (C-6), 18.4 (*C*(CH$_3$)$_3$), 25.1 (C-5), 26.0 (3C, C(*C*H$_3$)$_3$), 31.5 (C-7), 69.8 (C-8), 115.8 (C-3), 125.5 (C-4a), 148.4 (C-2), 155.2 (C-4), 161.9 (C-8a). FT-IR: $\tilde{\nu}$ [cm^{-1}] = 2951 (CH_3), 1531 (NO_2), 1350 (NO_2), 1250 (NO_2), 829 (Si–C). Purity (HPLC): 99% (t_r = 12.1 min).

4.1.5 8-(*tert*-Butyldimethylsilyloxy)-5,6,7,8-tetrahydroquinolin-4-amine (13)

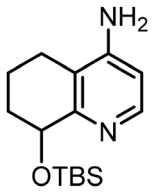

13

Pd/C (10 mol%, 43 mg) was added to a solution of nitro compound **12** (147 mg, 0.486 mmol) in dry EtOH (12 mL). The reaction atmosphere was changed to H_2 (1 bar, balloon) and the mixture was stirred at rt for 1 h. The reaction mixture was filtered over Celite®, the Celite® layer was washed with EtOH, and the filtrate was concentrated under vacuum, and the residue was purified by flash column chromatography (10 g cartridge, CH_2Cl_2/CH_3OH/*N*,*N*-dimethylaminoethanol 87/10/3). Colorless solid, mp 91 °C, yield 134 mg (99%). $C_{15}H_{26}N_2OSi$ (278.5 g mol^{-1}). TLC: R_f = 0.21 (ethyl acetate/cyclohexane 60/40). HR-MS (APCI): *m*/*z* = 279.1903 (calcd 279.1887 for $C_{15}H_{27}N_2OSi^+$ [M + H]$^+$). ^{1}H NMR (400 MHz, CD_3OD): δ (ppm) = 0.02 (s, 3H, Si-CH_3), 0.19 (s, 3H, Si-CH_3′), 0.87 (s, 9H, C(CH_3)$_3$), 1.75 (tt, *J* = 13.3/3.1 Hz, 1H, 7-CH_{ax}), 1.83 (dddd, *J* = 13.2/6.7/3.3/0.9 Hz, 1H, 6-CH_2), 1.98–2.03 (m, 1H, 7-CH_{eq}), 2.17 (dddd, *J* = 13.4/10.9/6.5/3.0 Hz, 1H, 6-CH_2), 2.34 (dddd, *J* = 16.8/10.9/6.8/0.8 Hz, 1H, 5-CH_{ax}), 2.53 (ddd, *J* = 16.8/6.5/2.4 Hz, 1H, 5-CH_{eq}), 4.69 (t, *J* = 3.3 Hz, 1H, 8-H), 6.54 (d, *J* = 5.7 Hz, 1H, 3-H), 7.87 (d, *J* = 5.7 Hz, 1H, 2-H). ^{13}C NMR (151 MHz, CD_3OD): δ (ppm) = −4.6 (Si-*C*H_3), −4.1 (Si-*C*H_3′), 17.1 (C-6), 19.0 (*C*(CH$_3$)$_3$), 23.3 (C-5), 26.4 (3C, C(*C*H$_3$)$_3$), 32.5 (C-7), 70.98 (C-8), 109.1 (C-3), 117.2 (C-4a), 146.4 (C-2), 155.3 (C-4), 156.4 (C-8a). FT-IR: $\tilde{\nu}$ [cm^{-1}] = 3456 (NH_2), 3333 (NH_2), 2940 (CH_3), 1628 (C=C_{arom}), 1022 (Si–O). Purity (HPLC): 97% (t_r = 19.7 min).

4.1.6 Methyl *N*-[8-(*tert*-butyldimethylsilyloxy)-5,6,7,8-tetrahydroquinolin-4-yl]carbamate (14a)

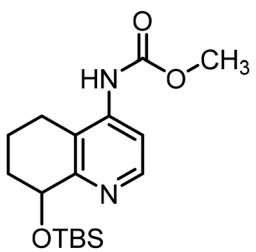

14a

. 1,1′-Carbonyldiimidazole (CDI, 88 mg, 0.54 mmol, 3.0 eq.) and DMAP (4 mg, 0.04 mmol, 0.2 eq.) were added to a solution of primary amine **13** (52 mg, 0.18 mmol, 1.0 eq.) in CH_3CN (1 mL). The mixture was stirred at 82 °C for 5 h. CH_3OH (0.3 mL, 7.4 mmol, 41 eq.) was added and the mixture was heated to reflux for 72 h. The mixture was concentrated under vacuum, water was added to the residue, and the aqueous layer was extracted with CH_2Cl_2 (3 × 15 mL). The combined organic layers were dried (Na_2SO_4) and filtered, the solvent was removed under vacuum, and the residue was purified by flash column chromatography (10 g cartridge, CH_2Cl_2/CH_3OH 98/2 → 95/5). Colorless solid, yield 51 mg (84%). $C_{17}H_{28}N_2O_3Si$ (336.5 g mol^{-1}). TLC: R_f = 0.50 (CH_2Cl_2/CH_3OH 95/5). HR-MS (APCI): m/z = 337.1965 (calcd 337.1942 for $C_{17}H_{29}N_2O_3Si^+$ [M + H]$^+$). ^{1}H NMR (600 MHz, $CDCl_3$): δ (ppm) = 0.03 (s, 3H, Si-CH_3), 0.21 (s, 3H, Si-CH_3′), 0.87 (s, 9H, C(CH_3)$_3$), 1.78 (tt, J = 13.2/3.2 Hz, 1H, 7-CH_{ax}), 1.81–1.87 (m, 1H, 6-CH_2), 1.99–2.05 (m, 1H, 7-CH_{eq}), 2.13–2.22 (m, 1H, 6-CH_2), 2.37–2.45 (m, 1H, 5-CH_{ax}), 2.59 (ddd, J = 16.0/6.2/3.0 Hz, 1H, 5-CH_{eq}), 3.80 (s, 3H, OCH_3), 4.79 (t, J = 3.5 Hz, 1H, 8-H), 6.60 (s, 1H, NH), 7.89 (d, J = 5.5 Hz, 1H, 3-H), 8.37 (d, J = 5.6 Hz, 1H, 2-H). ^{13}C NMR (151 MHz, $CDCl_3$): δ (ppm) = −4.8 (Si-CH$_3$), −4.0 (Si-CH$_3$′), 16.5 (C-6), 18.4 (C(CH$_3$)$_3$), 23.0 (C-5), 26.0 (3C, C(CH$_3$)$_3$), 31.5 (C-7), 52.8 (OCH$_3$), 70.0 (C-8), 111.6 (C-3), 118.8 (C-4a), 143.2 (C-4), 148.0 (C-2), 153.4 (C-8a), 157.9 (C=O). FT-IR: $\tilde{\nu}$ [cm^{-1}] = 3445 (N–H), 2947 (CH$_3$), 1748 (C=O), 1238 (C–N), 833 (Si–C).

4.1.7 *N*-[8-(*tert*-Butyldimethylsilyloxy)-5,6,7,8-tetrahydroquinolin-4-yl]acetamide (14b)

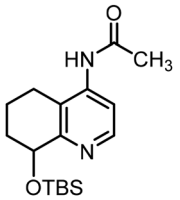

14b

A solution of primary amine **13** (0.746 g, 2.68 mmol) in acetic anhydride (8 mL) was stirred at 60 °C for 3 h. The mixture was concentrated under vacuum and the residue was purified by flash column chromatography (25 g cartridge, CH_2Cl_2/CH_3OH 98/2 to 94/6). To remove the remaining acetic acid, the product was dissolved in CH_2Cl_2 and the solution was washed with diluted aq. $NaHCO_3$. The aqueous layer was extracted with CH_2Cl_2 (1×) and the combined organic layers were dried (Na_2SO_4), filtered and concentrated under vacuum. Colorless solid, mp 98 °C, yield 0.848 g (99%). $C_{17}H_{28}N_2O_2Si$ (320.5 g mol^{-1}). TLC: R_f = 0.26 (CH_2Cl_2/CH_3OH 95/5). HR-MS (APCI): m/z = 321.1984 (calcd 321.1993 for $C_{17}H_{29}N_2O_2Si^+$ [M + H]$^+$). ^{1}H NMR (600 MHz, $CDCl_3$): δ (ppm) = 0.03 (s, 3H, Si-CH_3), 0.20 (s, 3H, Si-CH_3′), 0.87 (s, 9H, C(CH_3)$_3$), 1.78 (tt, J = 13.0/3.2 Hz, 1H, 7-CH_2), 1.82–1.87 (m, 1H, 6-CH_2), 2.00–2.05 (m, 1H, 7-CH_2), 2.15–2.21 (m, 1H, 6-CH_2), 2.22 (s, 3H, (NH(C=O)CH_3)), 2.46 (ddd, J = 16.3/10.5/6.5 Hz, 1H, 5-CH_{ax}), 2.63 (ddd, J = 16.0/6.3/3.0 Hz, 1H, 5-CH_{eq}), 4.80 (t, J = 3.5 Hz, 1H, 8-H), 7.06 (s, 1H, NH), 8.04 (s, broad, 1H, 3-H), 8.39 (d, J = 5.5 Hz, 1H, 2-H). ^{13}C NMR (151 MHz, $CDCl_3$): δ (ppm) = −4.6 (Si-CH$_3$′), −3.8 (Si-CH$_3$), 16.7 (C-6), 18.6 (C(CH$_3$)$_3$), 23.3 (C-5), 25.3 (NH(C=O)CH$_3$), 26.2 (3C, C(CH$_3$)$_3$), 31.7 (C-7), 70.2 (C-8), 113.8 (C-3), 119.6 (C-4a), 143.1 (C-4), 148.2 (C-2), 158.3 (C-8a), 168.7 (C=O). FT-IR: $\tilde{\nu}$ [cm^{-1}] = 2951 (CH$_3$), 1709 (C=O), 1578 (C=C$_{arom}$), 1250 (C–N), 833 (Si–C). Purity (HPLC): 98% (t_r = 19.2 min).

4.1.8 *tert*-Butyl *N*-[8-(*tert*-butyldimethylsilyloxy)-5,6,7,8-tetrahydroquinolin-4-yl]carbamate (14c)

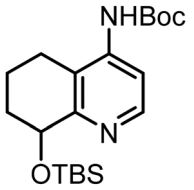

14c

Under a N_2 atmosphere, $(Boc)_2O$ (0.06 mL, 65 mg, 0.30 mmol, 1.2 eq.) and NEt_3 (0.04 mL, 0.30 mmol, 1.2 eq.) were added to a solution of primary amine **13** (71.4 mg, 0.251 mmol, 1.0 eq.) in CH_2Cl_2 (0.5 mL). The reaction mixture was stirred at 40 °C for 18 h. The volatiles were removed under reduced pressure and the crude product was purified repeatedly by flash column chromatography (10 g cartridge, CH_2Cl_2/CH_3OH 99/1 → 94/6). Yellow oil, yield 40.6 mg (43%), $C_{20}H_{34}N_2O_3Si$ (378.6 g mol^{-1}). TLC: R_f = 0.56 (CH_2Cl_2/CH_3OH 96/4). HR-MS (APCI): m/z = 379.2432 (calcd 379.2412 for $C_{20}H_{34}N_2O_3Si$ [M + H]$^+$). ^{1}H NMR (600 MHz, $CDCl_3$): δ (ppm) = 0.11 (d, J = 7.6 Hz, 3H, Si-CH$_3$), 0.24 (s, 3H, Si-CH$_3$′), 0.87 (s, 9H, SiC(CH_3)$_3$), 1.53 (s, 9H, OC(CH_3)$_3$), 1.77 (tt, J = 13.2/3.1 Hz, 1H, 7-CH$_2$), 1.88 (ddd, J = 13.6/6.7/3.4 Hz, 1H, 6-CH$_{eq}$), 1.99–2.08 (m, 1H, 7-CH$_2$), 2.20 (tddd, J = 13.2/10.1/6.5/3.1 Hz, 1H, 6-CH$_{ax}$), 2.44 (ddd, J = 16.5/10.4/6.6 Hz, 1H, 5-CH$_{ax}$), 2.63 (ddd, J = 16.3/6.4, 2.8 Hz, 1H, 5-CH$_{eq}$), 4.89–4.50 (m broad, 1H, 8-H), 6.62 (s, 1H, NH), 8.08 (d, J = 5.8 Hz, 1H, 3-H), 8.38 (d, J = 5.9 Hz, 1H, 2-H). ^{13}C NMR (151 MHz, $CDCl_3$): δ (ppm) = −4.7 (Si-CH$_3$), −3.9 (Si-CH_3′), 16.0 (C-6), 18.3 (SiC(CH$_3$)$_3$), 22.8 (C-5), 26.0 (3C, SiC(CH$_3$)$_3$), 28.3 (3C, OC(CH_3)$_3$), 31.0 (C-7), 68.5 (C-8), 82.5 (OC(CH$_3$)$_3$), 111.5 (C-3), 119.1 (C-4), 145.5[a] (C-2), 151.6 (C=O), 155.8[a] (C-8a). A signal for C-4a is not observed in the spectrum. [a]Signals are not observed in the spectrum but confirmed through 2D experiments. FT-IR: $\tilde{\nu}$ [cm^{-1}] = 2932 (CH$_3$), 1740 (C=O), 1578 (C=C), 1246 (Si–O–C), 833 (Si–C).

4.1.9 *N*-[8-(*tert*-Butyldimethylsilyloxy)-5,6,7,8-tetrahydroquinolin-4-yl]benzamide (14d)

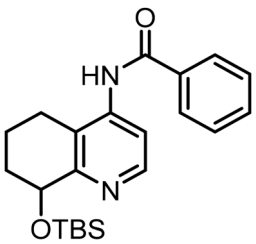

14d

. Benzoyl chloride (0.05 mL, 51 mg, 0.36 mmol, 1.0 eq.) was added to a solution of primary amine **13** (102 mg, 0.359 mmol, 1.0 eq.) and NEt_3 (0.05 mL, 0.36 mmol, 1.0 eq.) in a mixture of CH_3CN (1.0 mL) and CH_2Cl_2 (0.5 mL). The reaction mixture was stirred at rt. Additional benzoyl chloride (0.02 mL) was added after 4 h. After stirring for another 18 h, water was added, and the volatiles were removed under vacuum. The aqueous layer was extracted with CH_2Cl_2 (3 × 15 mL). The combined organic layers were dried (Na_2SO_4), filtered and evaporated under reduced pressure. The crude product was purified by flash column chromatography (25 g cartridge, CH_2Cl_2/CH_3OH 98/2 → 95/5). Off-white solid, yield 108 mg (78%), $C_{22}H_{30}N_2O_2Si$ (382.6 g mol^{-1}). TLC: R_f = 0.41 (CH_2Cl_2/ethyl acetate 95/5). HR-MS (APCI): m/z = 383.2139 (calcd 383.2149 for $C_{22}H_{31}N_2O_2Si$ [M + H]$^+$). ^{1}H NMR (600 MHz, $CDCl_3$): δ (ppm) = 0.12 (s, 3H, Si-CH_3'), 0.25 (s, 3H, Si-CH_3), 0.88 (s, 9H, C(CH_3)$_3$), 1.82 (tt, J = 13.2/3.1 Hz, 1H, 7-CH_2), 1.88–1.94 (m, 1H, 6-CH_2), 2.04–2.09 (m, 1H, 7-CH_2), 2.20–2.29 (m, 1H, 6-CH_2), 2.61 (ddd, J = 16.4/10.4/6.6 Hz, 1H, 5-CH_{ax}), 2.77 (ddd, J = 16.0/6.3/2.8 Hz, 1H, 5-CH_{eq}), 4.96 (s, 1H, 8-H), 7.51–7.55 (m, 2H, 3-H$_{Bz}$), 7.59–7.63 (m, 1H, 4-H$_{Bz}$), 7.86–7.90 (m, 2H, 2-H$_{Bz}$), 7.98 (s, 1H, NH), 8.35 (s, 1H, 3-H), 8.47 (d, J = 5.7 Hz, 1H, 2-H). ^{13}C NMR (151 MHz, $CDCl_3$): δ (ppm) = −4.7 (Si-CH_3), −3.9 (Si-CH_3'), 16.2 (C-6), 18.4 (C(CH_3)$_3$), 23.1 (C-5), 26.0 (3C, C(CH$_3$)$_3$), 31.1 (C-7), 68.8 (C-8), 113.7 (C-3), 120.5 (C-4a), 127.3 (2C, C-2$_{Bz}$, C-6$_{Bz}$), 129.3 (2C, C-3$_{Bz}$, C-5$_{Bz}$), 132.9 (C-4$_{Bz}$), 134.3 (C-1$_{Bz}$), 144.7 (C-4), 146.4 (C-2), 156.7 (C-8a), 165.7 (N(C=O)). FT-IR: $\tilde{\nu}$ [cm^{-1}] = 3306 (N–H), 2947 (C–H$_{aliph.}$), 1655 (C=O), 1516 (C–N), 837 (Si–C).

4.1.10 4-Acetamido-1-benzyl-8-(*tert*-butyldimethylsilyloxy)-5,6,7,8-tetrahydroquinolin-1-ium bromide (15b)

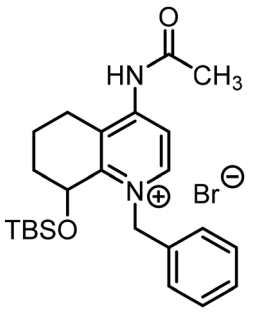

15b

Benzyl bromide (0.66 mL, 960 mg, 5.6 mmol, 1.1 eq.) was added to a solution of acetamide **14b** (1.63 g, 5.08 mmol, 1.0 eq.) in dry CH_3CN (16 mL). The reaction mixture was stirred at 40 °C for 40 h. The solvent was removed under reduced pressure, and the crude product was purified by reverse-phase flash column chromatography (30 g cartridge, water/CH_3CN 95/5 → 0/100). Colorless solid, yield 1.84 g (74%), $C_{24}H_{35}BrN_2O_2Si$ (491.5 g mol^{-1}). HR-MS (APCI): m/z = 369.2311(calcd 369.2357 for $C_{22}H_{33}N_2OSi^+$ [M–Ac–Br$^-$]$^+$). ^{1}H NMR (600 MHz, CD_3OD): δ (ppm) = 0.22 (s, 3H, Si-CH_3), 0.25 (s, 3H, Si-CH_3'), 0.93 (s, 9H, C(CH_3)$_3$), 1.81 (tt, J = 14.2/3.1 Hz, 1H, 7-CH_{ax}), 1.98–2.13 (m, 2H, 6-CH_2), 2.25–2.31 (m, 1H, 7-CH_{eq}), 2.37 (s, 3H, CH_3), 2.75–2.82 (m, 1H, 5-CH_{ax}), 3.04 (ddt, J = 17.6/5.6/1.6 Hz, 1H, 5-CH_{eq}), 5.20 (t, J = 3.0 Hz, 1H, 8-H), 5.80–5.92 (m broad, 2H, NCH_2Ph), 7.13–7.16 (m, 2H, 2-H$_{Bn}$, 6-H$_{Bn}$), 7.40–7.48 (m, 3H, 3-H$_{Bn}$, 4-H$_{Bn}$, 5-H$_{Bn}$), 8.54 (d, J = 7.3 Hz, 1H, 3-H), 8.83 (d, J = 7.3 Hz, 1H, 2-H). ^{13}C NMR (151 MHz, CD_3OD): δ (ppm) = −4.7 (Si-CH$_3$), −3.2 (Si-CH$_3'$), 15.6 (C-6), 19.1 (Si-C(CH$_3$)$_3$), 24.9 (CH$_3$), 25.0 (C-5), 26.3 (3C, Si-C(CH$_3$)$_3$), 30.8 (C-7), 59.2 (NCH_2Ph), 65.5 (C-8), 116.2 (C-3), 127.9 (2C, C-2$_{Bn}$, C-6$_{Bn}$), 130.2 (C-4$_{Bn}$), 130.8 (2C, C-3$_{Bn}$, C-5$_{Bn}$), 135.3 (C-1$_{Bn}$), 146.0 (C-2), 152.4 (C-8a), 153.7 (C-4), 172.8 (C=O). A signal for C-4a is not observed in the spectrum. FT-IR: $\tilde{\nu}$ [cm^{-1}] = 2951 (C–H$_{aliph.}$), 1720 (C=O), 1211 (C–N), 829 (Si–C).

4.1.11 1-Benzyl-4-[(*tert*-butoxycarbonyl)amino]-8-(*tert*-butyldimethylsilyloxy)-5,6,7,8-tetrahydroquinolin-1-ium bromide (15c)

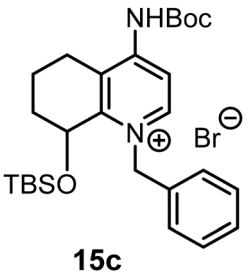

15c

Benzyl bromide (0.11 mL, 160 mg, 0.95 mmol, 1.2 eq.) was added to a solution of Boc derivative **14c** (300 mg, 0.792 mmol, 1.0 eq.) in dry CH_3CN (2 mL). The reaction mixture was stirred at 40 °C for 40 h. The solvent was removed under vacuum and the residue was purified by flash column chromatography (25 g cartridge, CH_2Cl_2/CH_3OH 97/3 → 90/10). Off-white solid, yield 387 mg (89%), $C_{27}H_{41}BrN_2O_3Si$ (549.7 g mol^{-1}). HR-MS (APCI): m/z = 469.2860 (calcd 469.2881 for $C_{27}H_{41}N_2O_3Si$ [M − Br$^-$]$^+$). Quinolinium salt **15c** was used in the next step without detailed characterization.

4.1.12 4-Benzamido-1-benzyl-8-(*tert*-butyldimethylsilyloxy)-5,6,7,8-tetrahydroquinolin-1-ium bromide (15d)

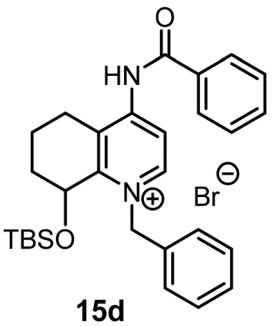

15d

Benzyl bromide (0.08 mL, 120 mg, 0.68 mmol, 1.3 eq.) was added to a solution of benzamide **14d** (209 mg, 0.547 mmol, 1.0 eq.) in a mixture of CH_3CN (1.5 mL) and CH_2Cl_2 (3 mL). The reaction mixture was stirred at 45 °C. Additional benzyl bromide (0.03 mL) was added after 16 h and after 72 h. After stirring for an additional 22 h, the volatiles were removed under reduced pressure and the residue was purified by flash column chromatography (25 g cartridge, CH_2Cl_2/CH_3OH 97/3

→ 93/7). Colorless oil, yield 303 mg (100%). $C_{29}H_{37}BrN_2O_2Si$ (553.6 g mol^{-1}). TLC: R_f = 0.21 (CH_2Cl_2/CH_3OH 95/5). HR-MS (APCI): m/z = 473.2635 (calcd 473.2619 for $C_{29}H_{37}N_2O_2Si^+$ [M − Br^-]$^+$). Quinolinium salt **15d** was used in the next step without detailed characterization.

4.1.13 *N*-[1-Benzyl-8-(*tert*-butyldimethylsilyloxy)-1,2,3,5,6,7,8,8a-octahydroquinolin-4-yl]acetamide (16b)

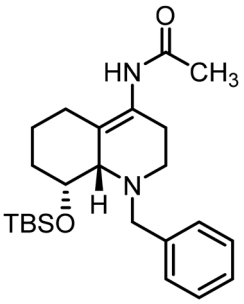

16b

Under a N_2 atmosphere, $NaBH_4$ (99 mg, 2.6 mmol, 4 eq.) was added to a cooled solution of quinolinium salt **15b** (269 mg, 0.546 mmol, 1 eq.) in dry CH_3OH (7 mL). The mixture was stirred at rt for 20 h and water was added. After removing CH_3OH under reduced pressure, the aqueous layer was extracted with ethyl acetate (3 × 10 mL). The combined organic layers were dried (Na_2SO_4) and filtered, and the solvent was removed under reduced pressure. The crude product was purified by flash column chromatography (25 g cartridge, CH_2Cl_2/CH_3OH 100/0 → 95/5). Yellow oil, yield 122 mg (54%), $C_{24}H_{38}N_2O_2Si$ (414.7 g mol^{-1}). TLC: R_f = 0.40 (CH_2Cl_2/CH_3OH 96/4). HR-MS (APCI): m/z = 415.2767 (calcd 415.2775 for $C_{24}H_{39}N_2O_2Si$ [M + H]$^+$). ^{1}H NMR (400 MHz, $CDCl_3$): δ (ppm) = 0.05–0.09 (m, 3H, Si-CH_3′), 0.13 (s, 3 × 0.55H, Si-CH_3), 0.15 (s, 3 × 0.45H, Si-CH_3*), 0.89 (s, 9 × 0.45H, C(CH_3)$_3$*), 0.91 (s, 9 × 0.55H, C(CH_3)$_3$), 1.38–1.55 (m, 2H, 5-CH_2, 5-CH_2*, 7-CH_2, 7-CH_2*), 1.62–1.78 (m, 3H, 5-CH_2′, 5-CH_2′*, 6-CH_2, 6-CH_2*, 7-CH_2′, 7-CH_2′*), 2.00 (s, 4 × 0.45H, 3-CH_2*, CH_3*), 2.04 (s, 3 × 0.55H, CH_3), 2.07 (m, 2 × 0.55H, 3-CH_2, 3-CH_2′), 2.38–2.57 (m, 2H, 2-CH_2, 2-CH_2*, 6-CH_2′, 3-CH_2′*), 2.72–2.79 (m, 0.45H, 6-CH_2′*), 2.83–2.89 (m broad, 1H, 8a-H), 3.16–3.26 (m, 1H, 2-CH_2′, 2-CH_2′*), 3.56 (d, J = 13.7 Hz, 0.45H, NCH_2Ph*), 3.60 (d, J = 13.6 Hz, 0.55H, NCH_2Ph) 3.85 (d, J = 13.7 Hz, 0.55H, NCH_2Ph), 3.90 (s, J = 13.7 Hz, 0.45H, NCH_2Ph*), 4.16–4.23 (m broad, 0.55H, 8-H), 4.28–4.34 (m broad, 0.45H, 8-H*), 6.16 (s, 0.55H, NH), 6.37 (s, 0.45H, NH*), 7.19–7.25 (m, 1H, 4-H_{Bn}), 7.27–7.39 (m, 4H, 2-H_{Bn}, 3-H_{Bn}, 5-H_{Bn}, 6-H_{Bn}). The ratio of rotamers is 55 : 45. The signals for the minor rotamer are marked with an asterisk (*). ^{13}C NMR (151 MHz, $CDCl_3$): δ (ppm) = −4.4 (0.45C, Si-CH$_3$′*), −4.23 (0.55C, Si-CH$_3$′), −4.20 (0.55C, Si-CH$_3$), −4.1 (0.45C, Si-CH$_3$*), 18.3 (1C, C(CH$_3$)$_3$), 20.0 (0.45C, CH$_3$*), 20.3 (0.45C, C-5*), 20.7 (0.55C, C-5), 23.9 (0.55C, CH$_3$), 26.06 (3 × 0.45C, C(CH$_3$)$_3$*), 26.12 (3 × 0.55C, C(CH$_3$)$_3$), 26.5 (0.45C, C-3*), 28.3 (0.45C, C-6*), 28.4 (0.55C, C-6), 29.4 (0.55C, C-3), 33.4 (0.45C, C-7*), 33.6 (0.55C, C-7), 46.5 (0.55C, C-2), 46.8 (0.45C, C-2*), 58.8 (0.45C, NCH$_2$Ph*), 58.9 (0.55C, NCH$_2$Ph), 64.8 (0.55C, C-8a), 65.3 (0.45C, C-8a*), 71.4 (0.45C, C-8*), 71.7 (0.55C, C-8), 125.8 (0.55C, C-4), 126.6 (0.45C, C-4*), 126.9 (0.55C, C-4$_{Bn}$), 127.1 (0.45C, C-4$_{Bn}$*), 127.6 (0.55C, C-4a), 128.2 (2 × 0.55C, C-3$_{Bn}$, C-5$_{Bn}$ or C-2$_{Bn}$, C-6$_{Bn}$), 128.4 (2 × 0.45C, C-3$_{Bn}$*, C-5$_{Bn}$* or C-2$_{Bn}$*, C-6$_{Bn}$*), 128.8 (2 × 0.45C, C-2$_{Bn}$*, C-6$_{Bn}$* or C-3$_{Bn}$*, C-5$_{Bn}$*), 128.9 (2 × 0.55C, C-2$_{Bn}$, C-6$_{Bn}$ or C-3$_{Bn}$, C-5$_{Bn}$), 133.9 (0.45C, C-4a*), 139.1 (0.45C, C-1$_{Bn}$*), 139.8 (0.55C, C-1$_{Bn}$), 168.3 (0.55C, N(*C*=O)), 173.2 (0.45C, N(*C*=O)*). The signals for the minor rotamer are marked with an asterisk (*). The C atoms of the benzyl ring (C-3$_{Bn}$/C-5$_{Bn}$ and C-2$_{Bn}$/C-6$_{Bn}$) cannot be reliably assigned with the present spectrum. FT-IR: $\tilde{\nu}$ [cm^{-1}] = 3252 (N–H$_{amide}$), 2951 and 2927 (C–H$_{aliph.}$), 1651 (C=O$_{amide}$), 1254 (C–N), 833 (Si–C).

4.1.14 *tert*-Butyl *N*-[1-benzyl-8-(*tert*-butyldimethylsilyloxy)-1,2,3,5,6,7,8,8a-octahydroquinolin-4-yl]carbamate (16c)

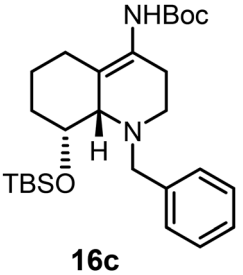

16c

$NaBH_4$ (117 mg, 3.17 mmol, 4.5 eq.) was added to a solution of quinolinium salt **15c** (387 mg, 0.705 mmol, 1.0 eq.) in dry CH_3OH (7 mL) at 0 °C. The reaction mixture was stirred at rt and additional $NaBH_4$ (13 mg, 0.35 mmol, 0.5 eq.) was added after 18 h and after an additional 4 h, respectively. After stirring for another 30 min, water was added to the reaction mixture and the volatiles were removed under vacuum. The aqueous layer was extracted with ethyl acetate (3 × 30 mL). The combined organic layers were dried (Na_2SO_4) and filtered, and the solvent was removed under reduced pressure. The crude product was purified by flash column chromatography (25 g cartridge, cyclohexane/ethyl acetate 99/1 → 90/10). Yellow oil, yield 268 mg (80%), $C_{27}H_{44}N_2O_3Si$ (472.7 g mol^{-1}). TLC: R_f = 0.53 (cyclohexane/ethyl acetate 90/10). HR-MS (APCI): m/z = 473.3178 (calcd 473.3194 for $C_{27}H_{45}N_2O_3Si$ [M + H]$^+$). Octahydroquinoline **16c** was used in the next step without detailed characterization.

4.1.15 *N*-[1-Benzyl-8-(*tert*-butyldimethylsilyloxy)-1,2,3,5,6,7,8,8a-octahydroquinolin-4-yl]benzamide (16d)

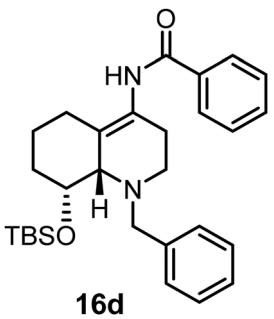

16d

Quinolinium salt **15d** (303 mg, 0.547 mmol, 1 eq.) was dissolved in CH_3OH (2.5 mL) and the solution was cooled to 0 °C. $NaBH_4$ (103 mg, 2.73 mmol, 5.0 eq.) was added to the solution and the reaction mixture was stirred at rt for 3.5 h. Water was added to the reaction mixture and CH_3OH was removed under reduced pressure. The aqueous layer was extracted with ethyl acetate (3 × 20 mL), dried (Na_2SO_4) and filtered, and the filtrate was concentrated under vacuum. The residue was purified by flash column chromatography (25 g cartridge, cyclohexane/ethyl acetate 90/10 → 70/30). Yellow solid, 164 mg (63%), $C_{29}H_{40}N_2O_2Si$ (476.7 g mol^{-1}). TLC: R_f = 0.41 (cyclohexane/ethyl acetate 80/20). HR-MS (APCI): m/z = 477.2879 (calcd 477.2932 for $C_{29}H_{41}N_2O_2Si$ [M + H]$^+$). Octahydroquinoline **16d** was used in the next step without detailed characterization.

4.1.16 Methyl *N*-[(4*RS*,4a*RS*,8*RS*,8a*SR*)-8-(*tert*-butyldimethylsilyloxy)decahydroquinolin-4-yl]carbamate (17a)

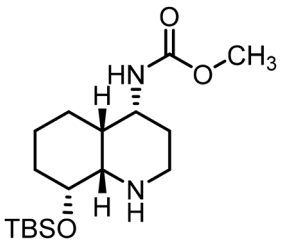

17a

Ru/C (1.849 g, 10 mol%) was added to a solution of carbamate **14a** (3.06 g, 9.15 mmol, 1 eq.) in i-PrOH (183 mL) and acetic acid (1.0 mL, 2 eq.). The atmosphere was changed to H_2 (50 bar) and the reaction mixture was stirred at 80 °C for 42 h. The mixture was filtered over Celite®, the Celite® layer was washed with CH_3OH, and the filtrate was concentrated under reduced pressure. The crude product was purified by flash column chromatography (50 g cartridge, CH_2Cl_2/CH_3OH w/5% NH_3 95/5 → 90/10). Colorless solid, mp 99 °C, yield 3.13 g (72%), $C_{17}H_{34}N_2O_3Si$ (342.6 g mol^{-1}). TLC: R_f = 0.45 (CH_2Cl_2/CH_3OH 90/10). HR-MS (APCI): m/z = 343.2437 (calcd 343.2412 for $C_{17}H_{35}N_2O_3Si^+$ [M + H]$^+$). ^{1}H NMR (600 MHz, CD_3OD): δ (ppm) = 0.09 (s, 3H, Si-CH_3), 0.10 (s, 3H, Si-CH_3′), 0.91 (s, 9H, C(CH_3)$_3$), 1.20–1.32 (m, 2H, 5-CH_{eq}, 6-CH_2), 1.48 (qd, J = 13.3/3.9 Hz, 1H, 5-CH_{ax}), 1.52–1.59 (m, 2H, 3-CH_2, 7-CH_2), 1.63–1.72 (m, 2H, 3-CH_2, 7-CH_2), 1.75–1.82 (m, 1H, 6-CH_2), 1.86–1.93 (m, 1H, 4a-H), 2.62–2.70 (m, 1H, 2-CH_{eq}), 2.84 (s broad, 1H, 8a-H), 3.14 (ddd, J = 11.5/4.4/2.5 Hz, 1H, 2-CH_{ax}), 3.58 (dt, J = 12.6/4.6 Hz, 1H, 4-H), 3.62 (s, 3H, CH_3), 3.72 (ddd, J = 11.4/5.0/3.9 Hz, 1H, 8-H). Signals for the NH protons are not observed in the spectrum. ^{13}C NMR (151 MHz, CD_3OD): δ (ppm) = −4.7 (Si-CH_3), −4.5 (Si-CH_3), 18.9 (C(CH$_3$)$_3$), 19.3 (C-5), 24.4 (C-6), 26.3 (3C, C(CH)$_3$)$_3$, 28.2 (C-3), 30.8 (C-7), 41.0 (C-4a), 46.7 (C-2), 52.3 (CH_3), 53.2 (C-4), 62.0 (C-8a), 74.3 (C-8), 158.7 (C=O). FT-IR: $\tilde{\nu}$ [cm^{-1}] = 3271 (N–H), 2928 (CH_3), 1713 (C=O), 1551 (N–H), 1258 (C–N).

4.1.17 *N*-[(4*RS*,4a*RS*,8*RS*,8a*SR*)-8-(*tert*-Butyldimethylsilyloxy)decahydroquinolin-4-yl] acetamide (17b)

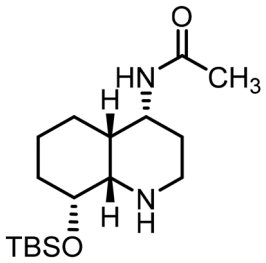

17b

Ru/C (0.158 g, 10 mol%) was added to a solution of acetamide **14b** (250 mg, 0.780 mmol, 1 eq.) in i-PrOH (15.5 mL) and acetic acid (0.1 mL, 2 eq.). The atmosphere was changed to H_2 (50 bar) and the reaction mixture was stirred at 80 °C for 42 h. The mixture was filtered over Celite®, the Celite® layer was washed with CH_3OH, and the filtrate was concentrated under reduced pressure. The crude product was purified by flash column chromatography (100 g cartridge, CH_2Cl_2/CH_3OH w/5% NH_3 95/5 → 85/15). Colorless solid, yield 196 mg (77%), $C_{17}H_{34}N_2O_2Si$ (326.6 g mol^{-1}). TLC: R_f = 0.16 (CH_2Cl_2/CH_3OH 90/10). HR-MS (APCI): m/z = 327.2450 (calcd 327.2462 for $C_{17}H_{35}N_2O_2Si$ [M + H]$^+$). ^{1}H NMR (600 MHz, CD_3OD): δ (ppm) = 0.14 (s, 3H, Si-CH_3′), 0.15 (s, 3H, Si-CH_3), 0.94 (s, 9H, C(CH_3)$_3$), 1.29–1.43 (m, 2H, 5-CH_2, 6-CH_2), 1.46–1.55 (m, 2H, 3-CH_2, 5-CH_2), 1.74–1.83 (m, 2H, 3-CH_2, 7-CH_2), 1.84–1.92 (m, 2H, 6-CH_2, 7-CH_2), 1.95 (s, 3H, CH_3), 2.18–2.24 (m, 1H, 4a-H), 3.05 (td, J = 13.0/3.4 Hz, 1H, 2-CH_2), 3.35 (t, J = 3.5 Hz, 1H, 8a-H), 3.43 (ddd, J = 12.7/4.5/2.2 Hz, 1H, 2-CH_2), 3.88 (dt, J = 11.8/4.6 Hz, 1H, 8-H), 4.02 (dt, J = 12.8/4.5 Hz, 1H, 4-H). Signals for the NH protons are not observed in the spectrum. ^{13}C NMR (151 MHz, CD_3OD): δ (ppm) = −4.7 (Si-CH_3′), −4.6 (Si-CH_3), 18.9 (C-5), 19.1 (C(CH$_3$)$_3$), 22.5 (CH_3), 23.4 (C-6), 25.3 (C-3), 26.4 (3C, C(CH$_3$)$_3$), 30.7 (C-7), 38.8 (C-4a), 45.8 (C-2), 49.6 (C-4), 61.9 (C-8a), 72.0 (C-8), 172.7 (C=O). FT-IR: $\tilde{\nu}$ [cm^{-1}] = 3248 (N–H$_{amide}$), 2943 and 2928 (C–H$_{aliph.}$), 1659 (C=O$_{amide}$), 1068 (Si–O), 833 (Si–C).

4.1.18 *tert*-Butyl *N*-[8-(*tert*-butyldimethylsilyloxy)decahydroquinolin-4-yl]carbamate (17c)

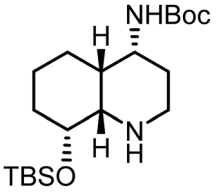

17c

Under a N_2 atmosphere, Pd/C (293 mg, 50 mol-%) was added to a solution of octahydroquinoline **16c** (256 mg, 0.541 mmol) in dry CH_3OH (7 mL). The atmosphere was changed to H_2 (5 bar) and the reaction mixture was stirred at rt for 120 h. The mixture was filtered over Celite®, the Celite® layer was washed with CH_3OH, and the filtrate was concentrated under reduced pressure. The crude product

was purified by flash column chromatography (10 g cartridge, CH_2Cl_2/CH_3OH 98/2 to 94/6). Reisolated octahydroquinoline **16c** (125 mg) was dissolved in dry CH_3OH (3 mL) and the solution was resubjected to the reduction conditions together with Pd/C (150 mg) for 10 d. The mixture was filtered over Celite®, the Celite® layer was washed with CH_3OH, and the filtrate was concentrated under reduced pressure. The crude product was combined with the previously isolated product and purified by flash column chromatography (10 g cartridge, CH_2Cl_2/CH_3OH 99/1 → 96/4). Colorless solid, yield 74.0 mg (36%), $C_{14}H_{26}N_2O_3$ (384.6 g mol^{-1}). TLC: R_f = 0.36 (CH_2Cl_2/MeOH 95/5). HR-MS (APCI): m/z = 386.2934 (calcd 386.2944 for $C_{14}H_{26}DN_2O_3$ $[M + D]^+$). The high-resolution mass spectrum was measured using an NMR sample dissolved in CD_3OD. ^{1}H NMR (600 MHz, CD_3OD): δ (ppm) = 0.08 (s, 3H, Si-CH_3), 0.09 (s, 3H, Si-CH_3'), 0.91 (s, 9H, SiC(CH_3)$_3$), 1.20–1.30 (m, 2H, 5-CH_{eq}, 6-CH_{ax}), 1.43 (s, 9H, OC(CH_3)$_3$), 1.45–1.57 (m, 3H, 3-CH_{eq}, 5-CH_{ax}, 7-CH_{eq}), 1.61–1.72 (m, 2H, 3-CH_{ax}, 7-CH_{ax}), 1.78 (dt, J = 13.7/3.5 Hz, 1H, 6-CH_{eq}), 1.89 (dt, J = 12.0/3.7 Hz, 1H, 4a-H), 2.65 (td, J = 12.0/2.8 Hz, 1H, 2-CH_{ax}), 2.83 (s broad, 1H, 8a-H), 3.13 (ddd, J = 11.4/4.4/2.4 Hz, 1H, 2-CH_{eq}), 3.52 (dt, J = 13.0/4.5 Hz, 1H, 4-H), 3.71 (dt, J = 11.4/4.4 Hz, 1H, 8-H). ^{13}C NMR (151 MHz, CD_3OD): δ (ppm) = −4.7 (Si-CH_3), −4.5 (Si-CH_3'), 18.9 (SiC(CH_3)$_3$), 19.4 (C-5), 24.5 (C-6), 26.3 (3C, SiC(CH_3)$_3$), 28.3 (C-3), 28.8 (3C, OC(CH_3)$_3$), 30.8 (C-7), 41.0 (C-4a), 46.7 (C-2), 52.8 (C-4), 62.1 (C-8a), 74.4 (C-8), 80.0 (OC(CH_3)$_3$), 157.7 (C=O). FT-IR: $\tilde{\nu}$ [cm^{-1}] = 3298 (N–H), 2928 (CH_3), 1674 (C=O), 1532 (N–H), 833 (Si–C).

4.1.19 *N*-[8-(*tert*-Butyldimethylsilyloxy)decahydroquinolin-4-yl]benzamide (17d)

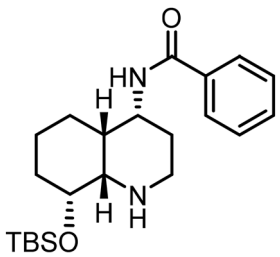

17d

Under a N_2 atmosphere, Pd/C (75 mg, 50 mol%) was added to a solution of octahydroquinoline **16d** (156 mg, 0.328 mmol) in CH_3OH (5 mL) and CH_2Cl_2 (0.2 mL). The atmosphere was changed to H_2 (5 bar) and the mixture was stirred at rt for 60 h. The mixture was filtered over Celite®, the Celite® layer was washed with CH_3OH, and the filtrate was concentrated under reduced pressure. The crude product was purified by flash column chromatography (25 g cartridge, CH_2Cl_2/CH_3OH 98/2 → 94/6). Colorless solid, yield 43 mg (34%), $C_{22}H_{36}N_2O_2Si$ (388.6 g mol^{-1}). TLC: R_f = 0.26 (CH_2Cl_2/MeOH 95/5). HR-MS (APCI): m/z = 389.2629 (calcd 389.2619 for $C_{22}H_{37}N_2O_2Si$ $[M + H]^+$). ^{1}H NMR (600 MHz, $CDCl_3$): δ (ppm) = 0.07 (s, 3H, CH_3'), 0.08 (s, 3H, CH_3), 0.89 (s, 9H, C(CH_3)$_3$), 1.19–1.28 (m, 1H, 6-CH_2), 1.28–1.34 (m, 1H, 5-CH_2), 1.53–1.61 (m, 1H, 7-CH_2), 1.71–1.85 (m, 4H, 3-CH_2, 5-CH_2, 6-CH_2, 7-CH_2), 1.85–1.96 (m, 1H, 3-CH_2), 2.09–2.16 (m broad, 1H, 4a-H), 2.80 (td, J = 11.9/2.8 Hz, 1H, 2-CH_2), 2.98 (s broad, 1H, 8a-H), 3.30–3.39 (m broad, 1H, 2-CH_2), 3.68 (dt, J = 11.0/4.4 Hz, 1H, 8-H), 4.20 (ddt, J = 12.8/8.6/4.6 Hz, 1H, 4-H), 6.11 (s, 1H, NH), 7.43 (ddt, J = 8.2/6.6/1.2 Hz, 2H, 3-H_{Ph}, 5-H_{Ph}), 7.48–7.52 (m, 1H, 4-H_{Ph}), 7.74–7.77 (m, 2H, 2-H_{Ph}, 6-H_{Ph}). Due to rotational isomerism, several signals appear as broad singlets or multiplets in the spectrum. ^{13}C NMR (151 MHz, $CDCl_3$): δ (ppm) = −4.6 (Si-CH_3'), −4.4 (Si-CH_3), 18.3 (3C, C(CH_3)$_3$), 18.8 (C-5), 23.4 (C-6), 26.0 (C(CH_3)$_3$), 27.5 (C-3), 29.8 (C-7), 39.1 (C-4a), 45.9 (C-2), 50.5 (C-4), 61.0 (C-8a), 72.6 (C-8), 127.0 (2C, C-2$_{Ph}$, C-6$_{Ph}$), 128.8 (2C, C-3$_{Ph}$, C-5$_{Ph}$), 131.7 (C-4$_{arom}$), 134.7 (C-1$_{arom}$), 166.9 (NH(C=O)). FT-IR: $\tilde{\nu}$ [cm^{-1}] = 3298 (N–H), 2928 (C–H$_{aliph.}$), 1635 (C=O), 1080 (Si–O), 833 (C–Si).

4.1.20 Methyl *N*-[(4*RS*,4a*RS*,8*RS*,8a*SR*)-8-hydroxydecahydroquinolin-4-yl]carbamate (18)

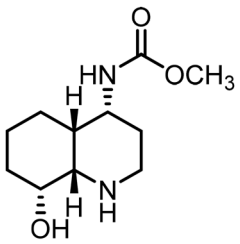

18

A solution of tetrabutylammonium fluoride (TBAF, 6.08 g, 19.3 mmol, 3 eq.) in anhydrous THF (32 mL) was added to a solution of methyl carbamate **17a** (2.20 g, 6.41 mmol, 1 eq.) in anhydrous THF (32 mL) and the reaction mixture was stirred at rt for 20 h. The solvent was removed under reduced pressure and the crude product was purified repeatedly by reverse-phase flash column chromatography (60 g RP cartridge, water/CH_3CN 98/2 → 0/100). Colorless solid, mp 185 °C, yield 1.54 g (100%), $C_{11}H_{20}N_2O_3$ (228.3 g mol^{-1}). TLC: R_f = 0.2 (CH_2Cl_2/CH_3OH 90/10). HR-MS (APCI): m/z = 229.1536 (calcd 229.1547 for $C_{11}H_{21}N_2O_3$ $[M + H]^+$). ^{1}H NMR (400 MHz, CD_3OD): δ (ppm) = 1.25–1.38 (m, 2H, 5-CH_2, 6-CH_2) 1.38–1.57 (m, 2H, 5-CH_2, 7-CH_2), 1.76–1.93 (m, 4H, 3-CH_2, 3-CH_2, 6-CH_2, 7-CH_2), 2.13–2.24 (m, 1H, 4a-H), 3.01 (td, J = 12.8/3.9 Hz, 1H, 2-CH_{ax}), 3.33–3.42 (m, 2H, 2-CH_{eq}, 8a-H), 3.64 (s, 3H, OCH_3), 3.72–3.85 (m, 2H, 4-H, 8-H). Signals for the OH and NH protons are not observed in the spectrum. ^{13}C NMR (101 MHz, CD_3OD): δ (ppm) = 18.8 (C-5), 23.5 (C-6), 25.3 (C-3), 29.7 (C-7), 38.9 (C-4a), 45.2 (C-2), 51.0 (C-4), 52.5 (OCH_3), 61.3 (C-8a), 69.5 (C-8), 158.6 (C=O). FT-IR: $\tilde{\nu}$ [cm^{-1}] = 3271 (O–H/N–H), 3071 (O–H/N–H), 2955 (CH_3), 1717 (C=O), 1562 (NH$_{deform}$), 1258 (C–N).

4.1.21 Methyl *N*-[(6*RS*,6a*RS*,9a*RS*,9b*SR*)-2,2-dioxo-5,6,6a,7,8,9,9a,9b-octahydro-4*H*-[1,2,3]oxathiazolo[5,4,3-ij] quinolin-

6-yl]carbamate (19)

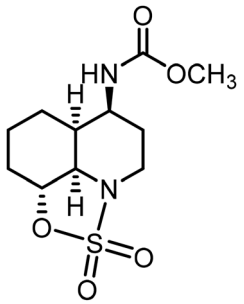

19

NEt_3 (0.55 mL, 3.9 mmol, 9 eq.) was added to a suspension of β-amino alcohol **18** (100 mg, 0.437 mmol, 1 eq.) and activated powdered molecular sieves in dry CH_3CN (0.75 mL). The suspension was stirred at rt for 1.5 h. A solution of SO_2Cl_2 (0.11 mL, 1.4 mmol, 3 eq.) in dry CH_3CN (2.0 mL) was added dropwise to the suspension at −25 °C. The reaction mixture was stirred at −25 °C for 30 min and at rt for 60 h. Water was added to the reaction mixture and the mixture was filtered. The filtrate was concentrated under vacuum and the crude material was purified by reverse-phase flash column chromatography (30 g cartridge, water/CH_3CN 95/5 → 0/100). Colorless solid, yield 62 mg (49%), $C_{11}H_{18}N_2O_5S$ (290.3 g mol^{-1}). TLC: R_f = 0.47 (CH_2Cl_2/CH_3OH 95/5). HR-MS (APCI): m/z = 291.0999 (calcd 291.1009 for $C_{11}H_{19}N_2O_5S^+$ $[M + H]^+$). ^1H NMR (400 MHz, CD_3OD): δ (ppm) = 1.19–1.34 (m, 1H, 8-CH_2), 1.41 (td, J = 12.8/2.9 Hz, 1H, 7-CH_{ax}), 1.46–1.54 (m, 1H, 7-CH_{eq}), 1.72–1.80 (m, 1H, 5-CH_2), 1.80–1.93 (m, 3H, 5-CH_2, 8-CH_2, 9-CH_2), 2.09–2.17 (m, 1H, 9-CH_2), 2.26 (ddt, J = 12.8/4.4/4.3 Hz, 1H, 6a-H), 2.81 (ddd, J = 12.4/11.2/3.3 Hz, 1H, 4-CH_{ax}), 3.48 (ddd, J = 11.2/4.7/2.4 Hz, 1H, 4-CH_{eq}), 3.64 (s, 3H, OCH_3), 3.66–3.75 (m, 2H, 6-H, 9b-H), 4.85–4.91 (m, 1H, 9a-H). A signal for the NH proton is not observed in the spectrum. ^{13}C NMR (101 MHz, CD_3OD): δ (ppm) = 19.5 (C-7), 22.3 (C-8), 25.9 (C-5), 29.4 (C-9), 39.3 (C-6a), 43.7 (C-4), 51.2 (C-9b), 52.5 (OCH_3), 60.3 (C-6), 83.7 (C-9a), 158.6 (N(*C*=O)). The signal for the C-atom of the *C*=O moiety is not observed in the spectrum but could be found through 2D experiments. FT-IR: $\tilde{\nu}$ [cm^{-1}] = 3414 (N–H), 2955 (C–H_{aliph}), 1721 (C=O), 1524 (N–H), 1180 (–SO_2).

4.1.22 Methyl *N*-[(4*RS*,4a*RS*,8*SR*,8a*SR*)-8-(pyrrolidin-1-yl) decahydroquinolin-4-yl]carbamate (20)

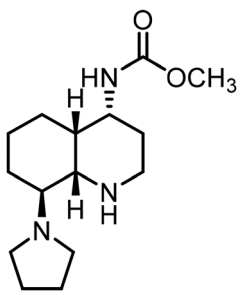

20

Pyrrolidine (2.3 mL, 1.9 g, 27 mmol, 30 eq.) was added to a suspension of oxathiazolidine **19** (265 mg, 0.91 mmol, 1.0 eq.) in CH_3CN (7 mL). The reaction mixture was stirred at 80 °C for 48 h. The volatiles were removed under vacuum and the residue was dissolved in ethyl acetate. Water (2 eq.) and TFA (2 eq.) were added until the solution was acidic. After stirring for 10 min at rt, pyrrolidine (2 eq.) was added and the volatiles were removed under vacuum. The crude product was purified by reverse-phase flash column chromatography (30 g RP cartridge, water/CH_3OH 99/1 → 0/100). Brown solid, yield 166 mg (65%), $C_{15}H_{27}N_3O_2$ (281.4 g mol^{-1}). TLC: R_f = 0.16 (CH_2Cl_2/CH_3OH w/5% NH_3 90/10). HR-MS (APCI): m/z = 282.2184 (calcd 282.2176 for $C_{15}H_{28}N_3O_2^+$ $[M + H]^+$). ^1H NMR (600 MHz, CD_3OD): δ (ppm) = 1.36–1.42 (m, 2H, 5-CH_2, 6-CH_2), 1.44–1.49 (m, 2H, 3-CH_2, 6-CH_2), 1.49–1.68 (m, 3H, 3-CH_2, 5-CH_2, 7-CH_2), 1.69–1.74 (m, 1H, 7-CH_2), 1.74–1.81 (m, 4H, N(CH_2CH_2)$_2$), 2.12–2.15 (m, 1H, 8-H), 2.19 (dt, J = 12.3/4.1 Hz, 1H, 4a-H), 2.51–2.61 (m, 4H, N(C$H_2$$CH_2$)$_2$), 2.65 (td, J = 12.8/3.1 Hz, 1H, 2-CH_{ax}), 2.91 (s broad, 1H, 8a-H), 3.09 (ddd, J = 12.9/4.6/2.1 Hz, 1H, 2-CH_{eq}), 3.55–3.64 (m, 4H, OCH_3, 4-H). Signals for the NH protons are not observed in the spectrum. ^{13}C NMR (151 MHz, CD_3OD): δ (ppm) = 19.8 (C-5), 20.7 (C-6), 24.3 (2C, N(CH_2CH_2)$_2$), 26.0 (C-7), 28.3 (C-3), 35.9 (C-4a), 46.9 (C-2), 52.3 (*C*H_3), 53.2 (2C, N(*C*$H_2$$CH_2$)$_2$), 53.3 (C-4), 58.4 (C-8a), 66.9 (C-8), 158.7 (C=O). FT-IR: $\tilde{\nu}$ [cm^{-1}] = 3302 (N–H), 2931 (C–H_{aliph}), 1690 (C=O), 1543 (N–H).

4.1.23 Methyl *N*-{[4*RS*,4a*RS*,8SR,8a*SR*]-1-[2-(3,4-dichlorophenyl)acetyl]-8-[pyrrolidin-1-yl]decahydroquinolin-4-yl} carbamate (6a)

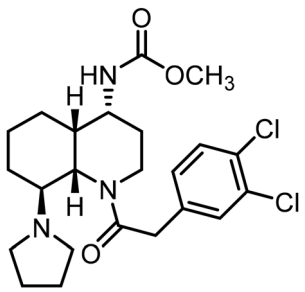

6a

N,*N*-Diisopropylethylamine (DIPEA, 0.5 mL, 2.9 mmol, 5 eq.) was added to a solution of secondary amine **20** (165 mg, 0.59 mmol, 1.0 eq.) in dry THF (12 mL). The solution was cooled to 0 °C and 2-(3,4-dichlorophenyl)acetyl chloride (**21a**, 146 mg, 0.65 mmol, 1.1 eq.) in dry THF (2 mL) was added. The reaction mixture was stirred at rt for 18 h. The volatiles were evaporated under vacuum and the residue was purified by flash column chromatography (25 g cartridge, CH_2Cl_2/CH_3OH 98/2 → 90/10). Colorless solid, yield 134 mg (49%), $C_{23}H_{31}Cl_2N_3O_3$ (468.4 g mol^{-1}). TLC: R_f = 0.38 (CH_2Cl_2/CH_3OH 90/10). HR-MS (APCI): m/z = 468.1720 (calcd 468.1815 for $C_{23}H_{32}{}^{35}Cl_2N_3O_3^+$ $[M + H]^+$). ^1H NMR (600 MHz, CD_3OD): δ (ppm) = 1.60 (dq, J = 14.1/2.7 Hz, 1H, 3-CH_{ax}), 1.63–1.78 (m, 5H, 3-CH_{eq}, 5-CH_2, 6-CH_2, 7-CH_2), 1.90–1.96 (m, 1H, 5-CH_2), 1.96–2.08 (m, 4H, N(CH_2CH_2)$_2$), 2.09–2.18 (m, 2H, 7-CH_2, 4a-H), 3.32–3.43 (m, 5H, 2-CH_2, N(C$H_2$$CH_2$)$_2$), 3.67 (s, 3H, OCH_3), 3.87–3.93 (m, 3H, 2-CH_2,

Ph-CH_2), 3.94–4.03 (m broad, 1H, 8-H), 4.07–4.11 (m broad, 1H, 4-H), 4.78–4.83 (m, 1H, 8a-H), 7.22 (dd, J = 8.2/2.1 Hz, 1H, 6-H_{Ph}), 7.48 (d, J = 8.3 Hz, 1H, 5-H_{Ph}), 7.49 (d, J = 2.1 Hz, 1H, 2-H_{Ph}). A signal for the N*H* proton is not observed in the spectrum. Due to rotational isomerism, several signals appear as broad multiplets in the spectrum. ^{13}C NMR (151 MHz, CD_3OD): δ (ppm) = 21.6 (C-6), 24.5 (C-7), 24.8 (2C, N(CH_2CH_2)$_2$), 28.5 (C-5), 32.6 (C-3), 38.8 (C-2), 39.2 (C-4a), 40.5 (Ph-CH_2), 49.6 (2C, N(CH_2CH_2)$_2$), 49.7 (C-4), 52.7 (OCH_3), 53.4 (C-8a), 60.1 (C-8), 130.7 (C-6$_{Ph}$), 131.5 (C-5$_{Ph}$), 131.9 (C-4$_{Ph}$), 132.8 (C-2$_{Ph}$), 133.2 (C-3$_{Ph}$), 137.2 (C-1$_{Ph}$), 159.3 (NH(C=O)OCH_3), 173.4 (N(C=O)CH_2Ph). FT-IR: $\tilde{\nu}$ [cm^{-1}] = 3333 (N–H), 2955 (CH_3), 1724 (C=O$_{carbamate}$), 1612 (C=O$_{amide}$), 1528 (N–H). Purity (HPLC): 99% (t_r = 17.9 min). CCDC: 2514901.

4.1.24 Methyl *N*-{(4*RS*,4a*RS*,8*SR*,8a*SR*)-1-[2-(4-fluorophenyl)acetyl]-8-(pyrrolidin-1-yl)decahydroquinolin-4-yl}carbamate (6b)

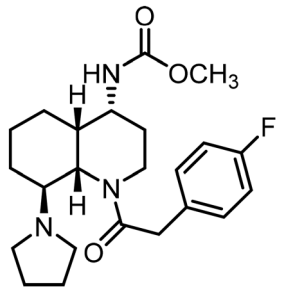

6b

2-(4-Fluorophenyl)acetic acid was transformed into the corresponding NHS-ester **21b** (see the SI, part 3). Under N_2, the NHS-ester **21b** (23 mg, 0.10 mmol, 1.1 eq.) was added to a solution of secondary amine **20** (25 mg, 0.09 mmol, 1.0 eq.) in dry THF (1 mL). After 5 min, a solution of Na_2CO_3 (28 mg, 0.27 mmol, 3.0 eq.) in water (0.5 mL) was added and the reaction mixture was stirred at rt for 18 h. The solvents were removed under vacuum and the residue was purified two times by flash column chromatography (10 g cartridge, CH_2Cl_2/CH_3OH with 5% NH_3 99/1 → 85/15). Colorless solid, yield 13 mg (36%), $C_{23}H_{32}FN_3O_3$ (417.5 g mol^{-1}). TLC: R_f = 0.65 (CH_2Cl_2/CH_3OH w/5% NH_3 98/2). HR-MS (APCI): m/z = 418.2446 (calcd 418.2500 for $C_{23}H_{33}{}^{19}FN_3O_3^+$ [M + H]$^+$). ^{1}H NMR (600 MHz, CD_3OD): δ (ppm) = 1.42–1.55 (m, 2H, 3-CH_2, 6-CH_2), 1.56–1.68 (m broad, 4H, 3-CH_2, 5-CH_2, 7-CH_2), 1.74–1.84 (m broad, 4H, N(CH_2CH_2)$_2$), 1.85–1.91 (m broad, 1H, 5-CH_2), 1.97–2.13 (m, 2H, 4a-H, 6-CH_2), 2.82–3.06 (m broad, 4H, N(CH_2CH_2)$_2$), 3.32–3.39 (m, 1H, 2-CH_2), 3.47–3.58 (m broad, 1H, 8-H), 3.65 (s, 3H, OCH_3), 3.69–3.91 (m, 3H, Ph-CH_2, 2-CH_2), 4.00 (s broad, 1H, 4-H), 4.61–4.78 (m broad, 1H, 8a-H), 7.02–7.07 (m, 2H, 3-H_{Ph}, 5-H_{Ph}), 7.29–7.33 (m, 2H, 2-H_{Ph}, 6-H_{Ph}). Due to rotational isomerism, several signals appear as broad singlets or multiplets in the spectrum. ^{13}C NMR (151 MHz, CD_3OD): δ (ppm) = 22.2 (C-7), 24.6 (2C, N(CH_2CH_2)$_2$), 25.0 (C-6), 28.9 (C-5), 32.9 (C-3), 39.1 (C-2), 39.6 (C-4a), 41.1 (Ph-CH_2), 49.9 (2C, N(CH_2CH_2)$_2$), 50.0 (C-4), 52.6 (CH_3), 54.6 (C-8a), 57.7 (C-8), 116.3 (d, 2C, J = 21.8 Hz, C-3$_{Ph}$, C-5$_{Ph}$), 131.8 (d, 2C, J = 7.9 Hz, C-2$_{Ph}$, C-6$_{Ph}$), 132.5 (C-1$_{Ph}$), 159.3 (NH(C=O)OCH_3), 163.2 (d, J = 244.0 Hz, C-4$_{Ph}$), 172.8 (N(C=O)CH_2Ph). Purity (HPLC): 99% (t_r = 15.4 min).

4.1.25 Methyl *N*-{[4*RS*,4a*RS*,8*SR*,8a*SR*]-1-[2-(pyridin-3-yl)acetyl]-8-[pyrrolidin-1-yl]decahydroquinolin-4-yl} carbamate (6c)

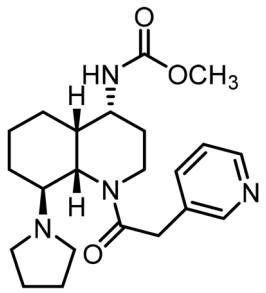

6c

2-(Pyridin-3-yl)acetic acid was transformed into the corresponding NHS-ester **21c** (see the SI, part 3). Under N_2, the NHS-ester **21c** (18.4 mg, 0.081 mmol, 1.1 eq.) was added to a solution of secondary amine **20** (20.8 g, 0.074 mmol, 1.0 eq.) in dry THF (1 mL). After 5 min, a solution of Na_2CO_3 (23.5 mg, 0.222 mmol, 3.0 eq.) in water (0.5 mL) was added and the reaction mixture was stirred at rt for 72 h. The solvents were removed under vacuum and the residue was purified two times by flash column chromatography (10 g cartridge, CH_2Cl_2/CH_3OH with 5% NH_3 98/2 to 85/15).

Colorless solid, yield 11.8 mg (40%), $C_{22}H_{32}N_4O_3$ (400.5 g mol^{-1}). HR-MS (APCI): m/z = 402.2570 (calcd 402.2610 for $C_{22}H_{32}DN_4O_3^+$ [M + D]$^+$). The high-resolution mass was measured using an NMR sample dissolved in CD_3OD. ^{1}H NMR (600 MHz, CD_3OD): δ (ppm) = 1.59–1.65 (m, 5H, C–H_{aliph}), 1.68–1.80 (m, 5H, N(CH_2CH_2)$_2$, C–H_{aliph}), 1.80–1.86 (m, 1H, C–H_{aliph}), 1.93 (d, J = 10.6 Hz, 1H, C–H_{aliph}), 2.10 (s, 1H, 4a-H), 2.77–2.94 (m broad, 4H, N(CH_2CH_2)$_2$), 3.66 (s, 3H, CH_3), 4.07 (s broad, 1H, 4-H), 7.40 (ddd, J = 7.9/4.9/0.9 Hz, 1H, 5-H_{Ph}), 7.78–7.82 (m, 1H, 6-H_{Ph}), 8.42 (dd, J = 4.9/1.6 Hz, 1H, 4-H_{Ph}), 8.47 (s, 1H, 2-H_{Ph}). Due to rotational isomerism and polar interactions with the deuterated solvent, strong signal broadening is observed in the spectrum. Protons close to the amide group, *i.e.*, 8-H, 8a-H, Ph-CH_2, and 2-CH_2, are therefore not observed in the spectrum. ^{13}C NMR (151 MHz, CD_3OD): δ (ppm) = 22.4 (CH_2), 24.7 (2C, N(CH_2CH_2)$_2$), 29.1 (CH_2), 33.2 (CH_2), 39.7 (C-4a), 49.6 (2C, N(CH_2CH_2)$_2$), 50.1 (C-4), 52.6 (CH_3), 125.1 (C-5$_{Ph}$), 133.7 (C-3$_{Ph}$), 139.2 (C-6$_{Ph}$), 148.3 (C-4$_{Ph}$), 150.8 (C-2$_{Ph}$), 159.4 (NH(C=O)OCH_3), 171.7 (N(C=O)CH_2Ph). Due to rotational isomerism and polar interactions with the deuterated solvent resulting in signal broadening, some carbon signals are not detected, and some carbon signals cannot be assigned in the spectrum. Purity (HPLC): 99.2% (t_r = 8.9 min).

4.1.26 Methyl *N*-[(4*RS*,4a*RS*,8*SR*,8a*SR*)-1-(3,4-dichlorobenzoyl)-8-(pyrrolidin-1-yl)decahydroquinolin-4-yl] carbamate (6d)

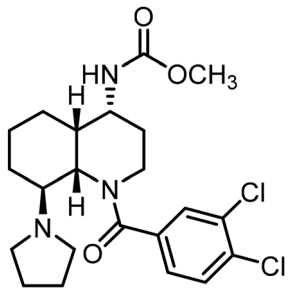

6d

3,4-Dichlorobenzoic acid was transformed into the corresponding NHS-ester **21d** (see the SI, part 3). Under N_2, the NHS-ester **21d** (26.6 mg, 0.097 mmol, 1.1 eq.) was added to a solution of secondary amine **20** (24.9 g, 0.089 mmol, 1.0 eq.) in dry THF (1 mL). After 5 min, a solution of Na_2CO_3 (28.2 mg, 0.267 mmol, 3.0 eq.) in water (0.5 mL) was added and the reaction mixture was stirred at rt for 18 h. An additional amount of NHS-ester (26.6 mg, 0.097 mmol, 1.1 eq.) was added and the reaction mixture was stirred at rt for an additional 24 h. The solvents were removed under vacuum and the residue was purified three times by flash column chromatography (10 g cartridge, CH_2Cl_2/CH_3OH with 5% NH_3 99/1 to 85/15). Colorless solid, yield 5.1 mg (13%), $C_{22}H_{29}Cl_2N_3O_3$ (454.4 g mol^{-1}). HR-MS (APCI): *m*/*z* = 454.1616 (calcd 454.1659 for $C_{22}H_{30}Cl_2N_3O_3^+$ $[M + H]^+$). ^{1}H NMR (600 MHz, CD_3OD): δ (ppm) = 1.57–1.70 (m broad, 5H, C–H_{aliph}), 1.73–1.85 (m broad, 5H, C–H_{aliph}), 1.94–2.06 (m, 5H, C–H_{aliph}), 2.32 (s broad, 1H, 4a-H), 2.51–2.67 (m, 1H), 2.75–3.04 (m broad, 4H, N(CH_2CH_2)$_2$), 3.34–3.41 (m, 1H, C–H_{aliph}), 3.67 (s, 3H, OCH_3), 4.15 (m broad, 1H, 4-H), 7.38 (dd, *J* = 8.3/2.0 Hz, 1H, 6-H_{Ph}), 7.63 (d, *J* = 8.3, 1H, 5-H_{Ph}), 7.66 (dd, *J* = 5.1/3.2 Hz, 1H, 2-H_{Ph}). Due to rotational isomerism and polar interactions with the deuterated solvent, strong signal broadening is observed in the spectrum. ^{13}C NMR (151 MHz, CD_3OD): δ (ppm) = 24.6 (CH_2), 28.9 (CH_2), 32.9 (CH_2), 39.5 (C-4a), 50.0 (C-4), 52.6 (CH_3), 127.7 (C-5$_{Ph}$), 130.4 (C-6$_{Ph}$), 131.9 (C-2$_{Ph}$), 133.7 (C-3$_{Ph}$), 134.9 (C-4$_{Ph}$), 137.9 (C-1$_{Ph}$), 171.4 (N(C=O)CH_2Ph). Due to rotational isomerism and polar interactions with the deuterated solvent resulting in signal broadening, some carbon signals are not detected, and some carbon signals cannot be assigned in the spectrum. Purity (HPLC): 97.5% (t_r = 17.2 min).

4.2. X-ray diffraction analysis

Data sets for compound **6a**·HCl were collected with a Bruker D8 Venture Photon III diffractometer using the following programs: data collection: APEX6 Version 2024.9-0;[44] cell refinement: SAINT Version 8.41;[44] data reduction: SAINT Version 8.41;[44] absorption correction: SADABS Version 2016/2;[44] structure solution: SHELXT Version 2018-3;[45] and structure refinement: SHELXL Version 2019-2.[46] *R* Values are given for observed reflections, and wR^2 values are given for all reflections.

Deposition number 2514901 (for compound **6a**·HCl) contains the supplementary crystallographic data for this paper.

4.3. Receptor binding studies

4.3.1. Determination of κ receptor affinity (guinea pig brain).[6,16] The assay was performed with the radioligand [^{3}H] U-69593 (55 Ci/mmol, Amersham, Little Chalfont, UK). The thawed guinea pig brain membrane preparation (about 100 μg of the protein) was incubated with various concentrations of the test compounds, 1 nM [^{3}H]U-69593, and TRIS-$MgCl_2$ buffer (50 mM, 8 mM $MgCl_2$, pH 7.4) at 37 °C. The non-specific binding was determined with 10 μM unlabeled U-69593. The K_d value of U-69593 is 0.69 nM.

4.3.2. Affinity towards other receptors. The assays used to determine the affinity towards μ and δ receptors are described in ref. 6 and 16. The assays used to determine the affinity towards σ_1 and σ_2 receptors are described in ref. 14 and 15. Experimental procedures for all receptor binding studies can be found in the SI.

4.4. Molecular docking

Modeling of receptor–ligand complexes was based on the crystal structure of the human κ receptor in the active state (PDB entry 6B73).[17] The structural model was prepared using the molecular operating environment 2022.02 (MOE, Chemical Computing Group, Montreal, Canada). Missing side chains and loops were added, and atom clashes were eliminated prior to docking. All docking experiments were performed with GOLD 5.2[47] by using the default settings and CHEMPLP as the primary scoring function. Residues within a distance of 11 Å around Asp138 were defined as the κ receptor binding site. Side-chain flexibilities were individually assessed and evaluated during pose selection. The most plausible docking poses were selected based on the assessment of 3D pharmacophore models built with LigandScout 4.4.3.[48]

4.5. Determination of log $D_{7.4}$ values, plasma protein binding and metabolic stability

Experimental details describing the determination of log $D_{7.4}$ values,[23,24] plasma protein binding[23,27,28] and metabolic stability[23,29] are given in the respective references.

4.6. Blood–brain permeability assay (PAMPA)

The assay was performed following a slightly modified procedure of Müller *et al.*[32]

In brief, 5 v/v% DMSO in MOPS buffer solutions (0.02 M, pH = 7.4) of each compound were first prepared at a final nominal concentration of 100 μM. These solutions were treated with ultrasonic waves for 1 min at room temperature and then centrifuged (2 min × 12 000*g*) in case the test compounds were insoluble at this concentration. Proceeding with saturated, homogeneous solutions ($C_D(0)$) is sufficient because log P_e only depends on relative concentrations. Each well of the top plate (MultiScreen MAIPNTR10; Millipore; Billerica, USA) was carefully coated with 5 μL of PBLE (porcine brain lipid extract, 141101, Avanti Polar Lipids, USA) solution in

n-dodecane/*n*-hexane (1 : 3) (10 w/v% with regard to *n*-dodecane), which was sonicated for 30 s to ensure solvation. After approximately 1 min, 150 μL of the $C_D(0)$ solution was added onto the membrane. The bottom plate (96-well collection plate, MATRNPS50; Millipore; Billerica, USA) was filled with 300 μL of MOPS buffer solution. The donor plate was carefully placed onto the acceptor plate, covered with a plate lid, and sealed with Parafilm to minimize evaporation. The plates were shaken and incubated at 37 °C for 4 h in a Thermomixer comfort (Eppendorf; Hamburg, Germany). After incubation, the PAMPA sandwich plates were separated and compound concentrations in the donor ($C_D(t)$) and acceptor ($C_A(t)$) solutions were determined by HPLC-MS (Shimadzu; Kyoto, Japan). The concentration of the donor solution at the zero time point ($C_D(0)$) was determined using the supernatant after centrifugation. Each compound was measured in three experimental replicates, and in each experimental replicate, each compound was administered in technical triplicate. Under iso-pH conditions, the effective permeability and the membrane retention of the drugs were calculated using the following equation:[49]

$$\log P_e = \log\frac{-2.303}{A\cdot(t-\tau_{SS})}\cdot\frac{(V_A\cdot V_D)}{(V_A+V_D)}\cdot\log\left[1-\left(\frac{V_A+V_D}{(1-MR)\cdot V_D}\right)\left(\frac{C_A(t)}{C_D(0)}\right)\right] \quad (1)$$

where P_e is the effective permeability coefficient (cm s^{-1}), A is the filter area (0.3 cm^2), V_D and V_A are the volumes of the donor (0.1 cm^3) and acceptor phases (0.1 cm^3), t is the incubation time (s), τ_{SS} is the time (s) required to reach steady state (240 s), $C_D(t)$ is the concentration (mol cm^{-3}) of the compound in the donor phase at time t, $C_A(t)$ is the concentration (mol cm^{-3}) of the compound in the acceptor phase at time t, $C_D(0)$ is the concentration (mol cm^{-3}) of the compound in the donor phase at time 0, and MR is the estimated membrane retention factor (the estimated mole fraction of solute lost to the membrane):

$$MR = \left(1-\frac{C_D(t)}{C_D(0)}-\frac{V_A}{V_D}\cdot\frac{C_A(t)}{C_D(0)}\right) \quad (2)$$

4.7. Flow cytometry of human PBMCs

Human PBMC samples were obtained from buffy coats collected from anonymous healthy donors (German Red Cross) with informed consent. Cells were isolated by Ficoll density gradient centrifugation. In some experiments, monocytes were separated using the Pan Monocyte Isolation kit, human, or the CD16+ Monocyte Isolation Kit, human, and the AutoMACS magnetic cell separator (all purchased from Miltenyi Biotec) according to the manufacturer's instructions. Subsequently, monocytes were cultured overnight at 37 °C and 5% CO_2 at a density of 1×10^6 cells per mL in RPMI medium supplemented with 2 mM L-glutamine, 100 U ml^{-1} penicillin–streptomycin, non-essential amino acids (NEAA, Seromed), 10% fetal calf serum (FCS), 10 mM HEPES buffer, 1 mM sodium pyruvate, and 500 μM β-mercaptoethanol to support optimal cell viability. Human monocytes were activated by adding eBioscience™ Lipopolysaccharide (LPS) Solution (Thermo Fisher Scientific, Waltham, MA) derived from *Escherichia coli* 026 : B6 at a concentration of 1 μg ml^{-1}. Twelve hours later, cells were treated with compounds **4**, **5**, and **6a** at a concentration of 10 μM or with the vehicle DMSO. Flow cytometry to assess relative cell numbers and the phenotype of the cells was performed 4 days after the addition of the κ agonists. Approximately 10^6 cells per sample were stained for 30 min in PBS in the dark using a live/dead marker according to the manufacturer's instructions (LIVE/DEAD™ Fixable Aqua Dead Cell Stain Kit; Thermo Fisher) and antibodies against HLA-DR (clone L243), CD14 (clone HCD14), CD16 (clone 3G8), CD44 (clone IM7), CD69 (clone FN50), and CD11b (clone M1/70), all purchased from BioLegend (San Diego, CA). After incubation, cells were washed twice with PBS, resuspended in PBS containing 0.1% FBS and acquired on a CytoFLEX LX cytometer using CytExpert acquisition software. Data analysis was performed using FlowJo (Becton Dickinson) or CytExpert software (Beckman Coulter). Dead cells were excluded from all analyses and doublets were discriminated using FSC-H *versus* FSC-A.

4.8. Cytokine quantification

Bead-based LEGENDplex™ analysis (BioLegend, San Diego, CA) was used to quantify cytokine concentrations in cell culture supernatants. In particular, the cytokines IL-1, IFN-γ, TNF, IL-6, IL-10, IL-12p70, and IL-18 were analyzed in human monocyte populations using the LEGENDplex™ Human Inflammation Panel 1 kit according to the manufacturer's instructions. Data were acquired on a Beckman Coulter CytoFLEX machine, and data acquisition or analysis were performed using the CytExpert and the Qognit software provided by BioLegend, respectively.

Conflicts of interest

The authors have no conflict of interest to declare.

Abbreviations

ADMET	Absorption, distribution, metabolism, elimination, toxicity
BBB	Blood–brain barrier
Cbz	Benzyloxycarbonyl
cHex	Cyclohexane
DIPEA	Diisopropylethylamine
DMEA	*N*,*N*-Dimethylethanamine
DMF	*N*,*N*-Dimethylformamide
DPPA	Diphenyl phosphoryl azide
DTG	Di-*o*-tolylguanidine

HATU	*O*-(7-Azabenzotriazol-1-yl)-*N*,*N*,*N*′,*N*′-tetramethyluronium hexafluorophosphate
HBA	H-bond acceptor groups
HBD	H-bond donor groups
HPAC	High-performance affinity chromatography
HPLC	High-performance liquid chromatography
IL-10	Interleukin-10
IL-18	Interleukin-18
INFγ	Interferon-γ
LLE	Ligand-lipophilicity efficiency
LPS	Lipopolysaccharide
*m*CPBA	*meta*-Chloroperbenzoic acid
MOPS	-(*N*-Morpholino)propanesulfonic acid
MR	Membrane retention factor
MS	Multiple sclerosis
MW	Molecular weight
NfκB	Nuclear factor κB
NK cells	Natural killer cells
NMR	Nuclear magnetic resonance spectroscopy
NOE	Nuclear Overhauser effect
PAMPA	Parallel artificial membrane permeability assay
PBLE	Porcine brain lipid extract
PBMC	Peripheral blood mononuclear cells
PDB	Protein Data Bank
P_e	Effective permeability coefficient
PPB	Plasma protein binding
SEM	Standard error of the mean
SL	Systemic lupus erythematosus (SLE)
THF	Tetrahydrofuran
TNFα	Tumor necrosis factor α
TPSA	Total polar surface area

Data availability

All data will be made available on request to the corresponding author of this paper.

Supplementary information (SI): general information used for the synthesis, HPLC method used to determine the purity of compounds, synthesis of activated acids for acylation of secondary amine **20**, X-ray crystal structure analysis of **6a**·HCl, NOE spectroscopy of decahydroquinoline **17a**, experimental procedures of receptor binding studies, ^{1}H and ^{13}C NMR spectra, HPLC chromatograms and HR-MS data of all test compounds and important intermediates. See DOI: https://doi.org/10.1039/d6ob00422a.

CCDC 2514901 contains the supplementary crystallographic data for this paper.[50]

Acknowledgements

We thank Arne Heusler and Marco Pierau for their advice and support in performing high-pressure hydrogenation experiments. This work was supported by the Deutsche Forschungsgemeinschaft, which is gratefully acknowledged.

References

1 C. Stein and H. Machelska, Modulation of peripheral sensory neurons by the immune system: implications for pain therapy, *Pharmacol. Rev.*, 2011, **63**(4), 860–881, DOI: 10.1124/pr.110.003145.

2 B. S. Kim, S. Inan, S. Ständer, T. Sciascia, J. C. Szepietowski and G. Yosipovitch, Role of kappa-opioid and mu-opioid receptors in pruritus: Peripheral and central itch circuits, *Exp. Dermatol.*, 2022, **31**(12), 1900–1907, DOI: 10.1111/exd.14669.

3 C. Du, Y. Duan, W. Wei, Y. Cai, H. Chai, J. Lv, X. Du, J. Zhu and X. Xie, Kappa opioid receptor activation alleviates experimental autoimmune encephalomyelitis and promotes oligodendrocyte-mediated remyelination, *Nat. Commun.*, 2016, **7**(1), 11120, DOI: 10.1038/ncomms11120.

4 F. Mei, S. R. Mayoral, H. Nobuta, F. Wang, C. Desponts, D. S. Lorrain, L. Xiao, A. J. Green, D. Rowitch, J. Whistler and J. R. Chan, Identification of the Kappa-Opioid Receptor as a Therapeutic Target for Oligodendrocyte Remyelination, *J. Neurosci.*, 2016, **36**(30), 7925–7935, DOI: 10.1523/JNEUROSCI.1493-16.2016.

5 B. Martin, D. Schepmann, F. A. Bernal, T. J. Schmidt, T. Che, K. Loser and B. Wünsch, Enantiomerically Pure Quinoline-Based κ-Opioid Receptor Agonists: Chemoenzymatic Synthesis and Pharmacological Evaluation, *ChemMedChem*, 2020, **15**(15), 1408–1420, DOI: 10.1002/cmdc.202000300.

6 C. Bourgeois, E. Werfel, F. Galla, K. Lehmkuhl, H. Torres-Gómez, D. Schepmann, B. Kögel, T. Christoph, W. Straßburger, W. Englberger, M. Soeberdt, S. Hüwel, H.-J. Galla and B. Wünsch, Synthesis and pharmacological evaluation of 5-pyrrolidinylquinoxalines as a novel class of peripherally restricted κ-opioid receptor agonists, *J. Med. Chem.*, 2014, **57**(15), 6845–6860, DOI: 10.1021/jm500940q.

7 P. Molenveld, R. Des Bouzanne Mazery, G. J. Sterk, R. P. M. Storcken, R. Autar, B. van Oss, R. N. S. van der Haas, R. Fröhlich, D. Schepmann, B. Wünsch and M. Soeberdt, Conformationally restricted κ-opioid receptor agonists: Synthesis and pharmacological evaluation of diastereoisomeric and enantiomeric decahydroquinoxalines, *Bioorg. Med. Chem. Lett.*, 2015, **25**(22), 5326–5330, DOI: 10.1016/j.bmcl.2015.09.040.

8 B. R. de Costa, W. D. Bowen, S. B. Hellewell, C. George, R. B. Rothman, A. A. Reid, J. M. Walker, A. E. Jacobson and K. C. Rice, Alterations in the stereochemistry of the kappa-selective opioid agonist U50,488 result in high-affinity sigma ligands, *J. Med. Chem.*, 1989, **32**(8), 1996–2002, DOI: 10.1021/jm00128a050.

9 V. Vecchietti, A. Giordani, G. Giardina, R. Colle and G. D. Clarke, (2S)-1-(arylacetyl)-2-(aminomethyl)piperidine derivatives: novel, highly selective kappa opioid analgesics, *J. Med. Chem.*, 1991, **34**(1), 397–403, DOI: 10.1021/jm00105a061.

10 P. F. Vonvoigtlander and R. A. Lewis, Analgesic and mechanistic evaluation of spiradoline, a potent kappa

opioid, *J. Pharmacol. Exp. Ther.*, 1988, **246**(1), 259–262, DOI: 10.1016/s0022-3565(25)21012-6.

11 L. Lückemeier, M. Pierau and F. Glorius, Asymmetric arene hydrogenation: towards sustainability and application, *Chem. Soc. Rev.*, 2023, **52**(15), 4996–5012, DOI: 10.1039/D3CS00329A.

12 M. P. Wiesenfeldt, Z. Nairoukh, T. Dalton and F. Glorius, Selective Arene Hydrogenation for Direct Access to Saturated Carbo- and Heterocycles, *Angew. Chem., Int. Ed.*, 2019, **58**(31), 10460–10476, DOI: 10.1002/anie.201814471.

13 F. I. Carroll, P. Abraham, K. Parham, X. Bai, X. Zhang, G. A. Brine, S. W. Mascarella, B. R. Martin, E. L. May and C. Sauss, Enantiomeric N-substituted N-normetazocines: a comparative study of affinities at sigma, PCP, and mu opioid receptors, *J. Med. Chem.*, 1992, **35**(15), 2812–2818, DOI: 10.1021/jm00093a014.

14 P. Hasebein, B. Frehland, K. Lehmkuhl, R. Fröhlich, D. Schepmann and B. Wünsch, Synthesis and pharmacological evaluation of like- and unlike-configured tetrahydro-2-benzazepines with the α-substituted benzyl moiety in the 5-position, *Org. Biomol. Chem.*, 2014, **12**(29), 5407–5426, DOI: 10.1039/C4OB00510D.

15 C. Meyer, B. Neue, D. Schepmann, S. Yanagisawa, J. Yamaguchi, E.-U. Würthwein, K. Itami and B. Wünsch, Improvement of σ1 receptor affinity by late-stage C-H-bond arylation of spirocyclic lactones, *Bioorg. Med. Chem.*, 2013, **21**(7), 1844–1856, DOI: 10.1016/j.bmc.2013.01.038.

16 C. Wittig, D. Schepmann, M. Soeberdt, C. G. Daniliuc and B. Wünsch, Stereoselective synthesis of conformationally restricted KOR agonists based on the 2,5-diazabicyclo2.2.2octane scaffold, *Org. Biomol. Chem.*, 2017, **15**(31), 6520–6540, DOI: 10.1039/C7OB01530E.

17 T. Che, S. Majumdar, S. A. Zaidi, P. Ondachi, J. D. McCorvy, S. Wang, P. D. Mosier, R. Uprety, E. Vardy, B. E. Krumm, G. W. Han, M.-Y. Lee, E. Pardon, J. Steyaert, X.-P. Huang, R. T. Strachan, A. R. Tribo, G. W. Pasternak, F. I. Carroll, R. C. Stevens, V. Cherezov, V. Katritch, D. Wacker and B. L. Roth, Structure of the Nanobody-Stabilized Active State of the Kappa Opioid Receptor, *Cell*, 2018, **172**(1–2), 55–67, DOI: 10.1016/j.cell.2017.12.011.

18 O. Suno-Ikeda, C. Nishikawa, R. Suzuki, S. Yokoi, S. Iwata, T. Takai, T. Ogura, M. Hirose, A. Tokuda, R. Katamoto, A. Inoue, E. Asai, R. Kise, Y. Sugita, T. Kato, H. Nagase, A. Mitsutake, T. Saitoh, K. Katayama, A. Inoue, H. Kandori, T. Kobayashi and R. Suno, Structural and dynamic insights into the biased signaling mechanism of the human kappa opioid receptor, *Nat. Commun.*, 2025, **16**, 9392, DOI: 10.1038/s41467-025-64882-1.

19 J. Hoffmann, D. Schepmann, C. Daniliuc, M. Bermudez and B. Wünsch, Stereoselective synthesis and biological evaluation of perhydroquinoxaline-based κ receptor agonists, *Int. J. Mol. Sci.*, 2025, **26**(3), 998, DOI: 10.3390/ijms26030998.

20 L. Flämig, T. Schidelko, L. Blicker, K. Hoffmann, C. Daniliuc, D. Schepmann, M. Bermúdez, K. Loser and B. Wünsch, Chiral pool synthesis of enantiomerically pure morphan derivatives with κ receptor affinity from (*S*)-perillaldehyde, *Eur. J. Med. Chem.*, 2026, **301**, 118218, DOI: 10.1016/j.ejmech.2025.118218.

21 N. P. Doering, K. Puls, M. Diceglie, A. Meraner, A. Hentsch, S. Hongnak, A. Wurzer, H. Schmidhammer, M. Spetea, M. Nazare and G. Wolber, Mechanistic Insights into G Protein-Biased κ-Opioid Receptor Signaling Using Dual-Charged Naltrexamine Amides, *J. Med. Chem.*, 2026, **69**, 3833–3851, DOI: 10.1021/acs.jmedchem.5c02135.

22 A. Abdelwaly, H. Safwan, S. Chatterjee, M. Elsayed, K. M. Darwish5, A. Chittiboyina and M. A. Helal, Novel dual kappa/mu opioid ligands based on a tetrahydroisoquinoline-valine hybrid nucleus, *Sci. Rep.*, 2025, **15**, 36138, DOI: 10.1038/s41598-025-08398-0.

23 F. Börgel, F. Galla, K. Lehmkuhl, D. Schepmann, S. M. Ametamey and B. Wünsch, Pharmacokinetic properties of enantiomerically pure GluN2B selective NMDA receptor antagonists with 3-benzazepine scaffold, *J. Pharm. Biomed. Anal.*, 2019, **172**, 214–222, DOI: 10.1016/j.jpba.2019.04.032.

24 F. Galla, C. Bourgeois, K. Lehmkuhl, D. Schepmann, M. Soeberdt, T. Lotts, C. Abels, S. Ständer and B. Wünsch, Effects of polar κ receptor agonists designed for the periphery on ATP-induced Ca 2+ release from keratinocytes, *Med. Chem. Commun.*, 2016, **7**(2), 317–326, DOI: 10.1039/C5MD00414D.

25 P. D. Leeson and B. Springthorpe, The influence of drug-like concepts on decision-making in medicinal chemistry, *Nat. Rev. Drug Discovery*, 2007, **6**(11), 881–890, DOI: 10.1038/nrd2445.

26 A. Tarcsay, K. Nyíri and G. M. Keseru, Impact of lipophilic efficiency on compound quality, *J. Med. Chem.*, 2012, **55**(3), 1252–1260, DOI: 10.1021/jm201388p.

27 V. Butsch, F. Börgel, F. Galla, K. Schwegmann, S. Hermann, M. Schäfers, B. Riemann, B. Wünsch and S. Wagner, Design, (Radio)Synthesis, and in Vitro and in Vivo Evaluation of Highly Selective and Potent Matrix Metalloproteinase 12 (MMP-12) Inhibitors as Radiotracers for Positron Emission Tomography, *J. Med. Chem.*, 2018, **61**(9), 4115–4134, DOI: 10.1021/acs.jmedchem.8b00200.

28 C. P. Konken, K. Heßling, I. Thale, S. Schelhaas, J. Dabel, S. Maskri, E. Bulk, T. Budde, O. Koch, A. Schwab, M. Schäfers and B. Wünsch, Imaging of the calcium activated potassium channel 3.1 (KCa 3.1) in vivo using a senicapoc-derived positron emission tomography tracer, *Arch. Pharm.*, 2022, **355**(12), e2200388, DOI: 10.1002/ardp.202200388.

29 C. Wiese, E. Große Maestrup, F. Galla, D. Schepmann, A. Hiller, S. Fischer, F.-A. Ludwig, W. Deuther-Conrad, C. K. Donat, P. Brust, L. Büter, U. Karst and B. Wünsch, Comparison of in Silico, Electrochemical, in Vitro and in Vivo Metabolism of a Homologous Series of (Radio)fluorinated σ1 Receptor Ligands Designed for Positron Emission Tomography, *ChemMedChem*, 2016, **11**(21), 2445–2458, DOI: 10.1002/cmdc.201600366.

30 L. Di, E. H. Kerns, I. F. Bezar, S. L. Petusky and Y. Huang, Comparison of blood-brain barrier permeability assays:

in situ brain perfusion, MDR1-MDCKII and PAMPA-BBB, *J. Pharm. Sci.*, 2009, **98**(6), 1980–1991, DOI: 10.1002/jps.21580.

31 L. Di, E. H. Kerns, K. Fan, O. J. McConnell and G. T. Carter, High throughput artificial membrane permeability assay for blood-brain barrier, *Eur. J. Med. Chem.*, 2003, **38**(3), 223–232, DOI: 10.1016/S0223-5234(03)00012-6.

32 J. Müller, K. Esső, G. Dargó, Á. Könczöl and G. T. Balogh, Tuning the predictive capacity of the PAMPA-BBB model, *Eur. J. Pharm. Sci.*, 2015, **79**, 53–60, DOI: 10.1016/j.ejps.2015.08.019.

33 A. Daina, O. Michielin and V. Zoete, SwissADME: a free web tool to evaluate pharmacokinetics, drug-likeness and medicinal chemistry friendliness of small molecules, *Sci. Rep.*, 2017, **7**, 42717, DOI: 10.1038/srep42717.

34 M. Guilliams, A. Mildner and S. Yona, Developmental and Functional Heterogeneity of Monocytes, *Immunity*, 2018, **49**(4), 595–613, DOI: 10.1016/j.immuni.2018.10.005.

35 C. Shi and E. G. Pamer, Monocyte recruitment during infection and inflammation, *Nat. Rev. Immunol.*, 2011, **11**(11), 762–774, DOI: 10.1038/nri3070.

36 T. S. Kapellos, L. Bonaguro, I. Gemünd, N. Reusch, A. Saglam, E. R. Hinkley and J. L. Schultze, Human Monocyte Subsets and Phenotypes in Major Chronic Inflammatory Diseases, *Front. Immunol.*, 2019, **10**, 2035, DOI: 10.3389/fimmu.2019.02035.

37 A. Ożańska, D. Szymczak and J. Rybka, Pattern of human monocyte subpopulations in health and disease, *Scand. J. Immunol.*, 2020, **92**(1), e12883, DOI: 10.1111/sji.12883.

38 A. Szczepaniak, W. Machelak, J. Fichna and M. Zielińska, The role of kappa opioid receptors in immune system - An overview, *Eur. J. Pharmacol.*, 2022, **933**, 175214, DOI: 10.1016/j.ejphar.2022.175214.

39 M. L. Dalefield, B. Scouller, R. Bibi and B. M. Kivell, The Kappa Opioid Receptor: A Promising Therapeutic Target for Multiple Pathologies, *Front. Immunol.*, 2022, **13**, 837671, DOI: 10.3389/fphar.2022.837671.

40 R. Mukherjee, P. Kanti Barman, P. Kumar Thatoi, R. Tripathy, B. Kumar Das and B. Ravindran, Non-Classical monocytes display inflammatory features: Validation in Sepsis and Systemic Lupus Erythematous, *Sci. Rep.*, 2015, **5**, 13886, DOI: 10.1038/srep13886.

41 M. Tsukamoto, N. Seta, K. Yoshimoto, K. Suzuki, K. Yamaoka and T. Takeuchi, CD14brightCD16+ intermediate monocytes are induced by interleukin-10 and positively correlate with disease activity in rheumatoid arthritis, *Arthritis Res. Ther.*, 2017, **19**(1), 28, DOI: 10.1186/s13075-016-1216-6.

42 H. Xu, A. Manivannan, I. Crane, R. Dawson and J. Liversidge, Critical but divergent roles for CD62L and CD44 in directing blood monocyte trafficking in vivo during inflammation, *Blood*, 2008, **112**(4), 1166–1174, DOI: 10.1182/blood-2007-06-098327.

43 M. Soeberdt, P. Molenveld, R. P. M. Storcken, R. Des Bouzanne Mazery, G. J. Sterk, R. Autar, M. G. Bolster, C. Wagner, S. N. H. Aerts, F. R. van Holst, A. Wegert, G. Tangherlini, B. Frehland, D. Schepmann, D. Metze, T. Lotts, U. Knie, K.-Y. Lin, T.-Y. Huang, C.-C. Lai, S. Ständer, B. Wünsch and C. Abels, Design and Synthesis of Enantiomerically Pure Decahydroquinoxalines as Potent and Selective κ-Opioid Receptor Agonists with Anti-Inflammatory Activity in Vivo, *J. Med. Chem.*, 2017, **60**(6), 2526–2551, DOI: 10.1021/acs.jmedchem.6b01868.

44 *APEX6 Version 2024.9-0, SAINT Version 8.41 and SADABS Bruker AXS area detector scaling and absorption correction Version 2016/2*, 2024.

45 G. M. Sheldrick, SHELXT - integrated space-group and crystal-structure determination, *AcActa Crystallogr., Sect. A: Found. Adv.*, 2015, **A71**(Pt 1), 3–8, DOI: 10.1107/S2053273314026370.

46 G. M. Sheldrick, Crystal structure refinement with SHELXL, *Acta Crystallogr., Sect. C: Struct. Chem.*, 2015, **C71**(1), 3–8, DOI: 10.1107/S2053229614024218.

47 G. Jones, P. Willett, R. C. Glen, A. R. Leach and R. Taylor, Development and validation of a genetic algorithm for flexible docking, *J. Mol. Biol.*, 1997, **267**(3), 727–748, DOI: 10.1006/jmbi.1996.0897.

48 G. Wolber and T. Langer, LigandScout: 3-D pharmacophores derived from protein-bound ligands and their use as virtual screening filters, *J. Chem. Inf. Model.*, 2005, **45**(1), 160–169, DOI: 10.1021/ci049885e.

49 A. Avdeef, *Absorption and Drug Development*, Wiley, 2012, DOI: 10.1002/9781118286067.

50 CCDC 2514901: Experimental Crystal Structure Determination, 2026, DOI: 10.5517/ccdc.csd.cc2qdyvy.